



Dottorato di Ricerca in
TERAPIE AVANZATE BIOMEDICHE E CHIRURGICHE

XXXV CICLO

Tesi di Dottorato

Coordinatore: Prof. Fabrizio Pane

*“Changes in markers of atherosclerosis and
multi-omic approach in patients with familial hypercholesterolemia treated with
PCSK9 inhibitors”*

Tutore:

Ch.mo Prof. Matteo Di Minno

Candidato:

Dott. Ilenia Lorenza Calcaterra

Anno Accademico 2021-2022

Index

1) Introduction:

- 1.1 Familial Hypercholesterolemia: genetics, clinical characteristics and cardiovascular risk;
- 1.2 Endothelial function and subclinical atherosclerosis;
- 1.3 Lipid lowering therapies: from statins to Proprotein convertase subtilisin/kexin type 9 (PCSK9) inhibitors;
- 1.4 Potential pleiotropic effects of PCSK9 inhibitors;
- 1.5 Project aim.

2) Methods:

- 2.1 Study protocol;
- 2.2 Blood and laboratory parameters;
- 2.3 Untargeted Lipidomic Analysis;
 - 2.3.1 Lipid extraction;
 - 2.3.2 UHPLC-ESI-Q-TOF-MS Analysis;
 - 2.3.3 Lipid Annotation and Data Analysis;
- 2.4 Untargeted Metabolomic Analysis;
 - 2.4.1 Untargeted LC-MS Metabolite Profiles;
 - 2.4.2 LC-MS Data Collection;
 - 2.4.3 Metabolites Identification;
- 2.5 Subclinical atherosclerosis markers;
 - 2.5.1 Brachial artery flow-mediated dilatation (FMD) with post-ischemic hyperemia (PIH);
 - 2.5.2 Carotid Stiffness and distensibility
- 2.6 Statistical Analysis;
- 2.7 Sample Size

3) Results:

- 3.1 Clinical and demographic
- 3.2 Serum cholesterol profile and lipoproteins levels after 4- and 12-Week Treatment
- 3.3 Effects of PCSK9 Inhibitor on Plasma Lipidome
- 3.4 Metabolomics Changes during Treatment with PCSK9 inhibitor

3.5 Carotid stiffness and distensibility

3.6 Oxidative stress markers

3.7 Endothelial function

4) Discussion

5) Conclusions

6) References

7) Acknowledgments

1.Introduction

1.1 Familial Hypercholesterolemia: genetics, clinical characteristics, and cardiovascular risk

Familial hypercholesterolemia (FH) is an autosomal dominant disorder, the frequency of the heterozygous FH (HeFH) has been estimated at 1 in 500 and of the homozygous FH (HoFH) at 1 in 1,000,000 individuals globally.^{1,2} However, in a recent meta-analysis estimated prevalence of FH was 1:250 and it could be classified as the most frequent genetic disease globally.³ FH is characterized by extremely high levels of circulating low-density lipoprotein cholesterol (LDL-C), a recognized major risk factor for atherosclerosis development and progression and for coronary artery disease (CAD); and for the presence of tendinous xanthomas and corneal arcus.⁴ The risk of premature CAD is increased to about 20-fold in heterozygous FH, with the highest risk being reported in young untreated men.^{1,5} Cases of valvular and supra-aortic stenosis due to lipid deposition have been reported in HoFH and rarely in HeFH.² FH is caused by mutations of different genes involved in LDL-C metabolism⁶. FH genetics is characterized by genetic heterogeneity, presence of variant clusters and phenotypic variability due to incomplete penetrance observed in some HeFH.⁷

In most cases, FH has dominant or co-dominant inheritance with over 90% penetrance and it is linked to mutations in LDLR, apolipoprotein B (APOB), and proprotein convertase subtilisin/kexin 9 (PCSK9) genes.⁶ However, an autosomal recessive form of FH caused by loss-of-function mutations in low-density lipoprotein receptor adaptor protein 1 (LDLRAP1), which encodes a protein required for clathrin-mediated internalization of the LDL receptor by liver cells, has also been documented.⁸ HeFH is caused by a pathogenic variant in one allele. In contrast, HoFH results from either biallelic mutations in one of the known genes (true homozygotes) or compound heterozygosity for two different mutations in the same or different candidate genes known to cause FH.^{5,7}

Mutations in *LDLR* gene were identified as a cause of FH in the 1970s and are the most frequently reported (>70 %).⁶ The gene for LDLR lies on the short arm of chromosome 19 (19p13.1–13.3).⁶ Defects noted in the LDLR can be classified into five broad categories: defective ligand binding, defective transport, defective internalization, recycling, and complete lack of receptors.⁸ At present, >2000 mutations from various centres have been identified and are available for review.^{7, 8}

APOB-100 is present on the LDL particle surface and serves as the ligand for the LDLR. Mutations in APOB (chromosome 2p23–24) have been identified in about 2–5 % of cases in northern Europe but have not been commonly noted in other populations.⁹ At present, 32 causative variants in APOB gene have been identified and are available for review.⁷ The APOB mutation that has been most commonly detected among northern Europeans is Arg3500Gln (haplotype inherited from a common ancestor 6000–7000 years ago).⁹ APOB mutations have been reported as having variable penetrance.¹

PCSK9 spans ~25kb on chromosomal region 1p32 and codes for a protein involved in LDL receptor degradation by post-transcription cell-surface interaction. Mutations leading to “gain” of function (GOF) of PCSK9 activity account for <5 % of cases of FH in most series.^{1, 7} “Loss” of function (LOF) mutations are associated with very low cholesterol levels and are protective against atherosclerosis.¹⁰⁻¹² At present, 23 causative variants in PCSK9 gene have been identified and are available for review.⁷ Recently, a mutation in signal transducing adaptor family member 1 (STAP 1) was associated with autosomal dominant FH.^{7, 13}

The autosomal recessive form of FH, first identified in the 1970s, and subsequently linked to the absent or non-functional expression of LDLRAP1 gene on chromosome 1p36–p35. This form of FH is quite rare, and most reported cases have come from Lebanon and Sardinia, Italy, and from consanguineous marriages.¹⁴ Heterozygotes for mutations in LDLRAP1 have normal lipid levels.¹⁴

Interestingly, data from several evidence shows that LDLR mutations show a gene dosage effect. LDL-C levels are roughly related to a genotype as follows: single heterozygous FH < double

heterozygote < homozygous APOB or PCSK9 gain-of-function mutation < homozygous LDLRAP1 or LDLR defective mutations < compound heterozygote: LDLR defective plus LDLR-negative (null) mutation < homozygous LDLR-negative (null) mutation.¹

Patients with very high LDL-C levels but no identifiable FH mutations are likely to have inherited a greater than average number of common lipid-raising variants of small effect (single nucleotide polymorphisms, SNPs) or have undiscovered gene(s).¹⁵ SNPs and polygenic contribution to lipid levels may also mostly account for variable penetrance noted in families (besides environmental factors, dietary influences, gene-environment interactions, epigenetic influences, and random variation).¹⁵ This may also explain milder phenotypes rarely seen with severe mutations.

Clinical characteristics of FH are well-defined three well-known formal criteria exist for diagnosing FH. These include the US MedPed (Make Early Diagnosis To Prevent Early Death) program, the Simon Broome Register Group in the UK,¹⁶ and the Dutch Lipid Clinic Network⁴ (**Figure 1**). Among these clinical scores, only the Simon Broome criteria can be used in children due to the use of specific cholesterol thresholds.

Dutch Lipid Clinic Network diagnostic criteria for familial hypercholesterolaemia (1) EAS  ESC 
European Society of Cardiology

Criteria	Points
1) Family history	
First-degree relative with known premature (men <55 years; women <60 years) coronary or vascular disease, or first-degree relative with known LDL-C above the 95th percentile	1
First-degree relative with tendinous xanthomata and/or arcus cornealis, or children <18 years of age with LDL-C above the 95th percentile	2
2) Clinical history	
Patient with premature (men <55 years; women <60 years) coronary artery disease	2
Patient with premature (men <55 years; women <60 years) cerebral or peripheral vascular disease	1
3) Physical examination*	
Tendinous xanthomata	6
Arcus cornealis before age 45 years	4
4) LDL-C levels (without treatment)	
LDL-C ≥8.5 mmol/L (≥325 mg/dL)	8
LDL-C 6.5–8.4 mmol/L (251–325 mg/dL)	5
LDL-C 5.0–6.4 mmol/L (191–250 mg/dL)	3
LDL-C 4.0–4.9 mmol/L (155–190 mg/dL)	1
5) DNA analysis	
Functional mutation in the LDLR, ApoB or PCSK9 genes	8
Choose only one score per group, the highest applicable (diagnosis is based on the total number of points obtained)	
A 'definite' FH diagnosis requires ≥8 points	
A 'probable' FH diagnosis requires 6–8 points	
A 'possible' FH diagnosis requires 3–5 points	

Figure 1: Dutch Lipid Clinic Network criteria for diagnosis of FH⁴

The above-mentioned criteria include evaluation about patient family history, cardiovascular (CV) events history and LDL-C levels. Doubtless, the presence of an FH-causative variant is a stand-

alone criterion to make a definite diagnosis of FH. Indeed, DNA testing provides the gold standard for FH diagnosis. However, it is noteworthy that a negative genetic test does not definitely exclude FH. Genetic testing may also be employed in cases without family contacts where FH is strongly suspected. The identification of the FH-causative variant has great relevance to perform cascade screening searching for the causative variant in family members increasing the number of diagnosed patients, above all the youngest ones who mostly benefit from early treatment.

The prognostic and clinical importance of genetic evaluation in patient with FH is highlighted by results of the study of Khera et al.¹⁷ showing that FH mutation status could also provide CAD risk information beyond that from a single LDL cholesterol measurement. Among 20,485 CAD-free control and prospective cohort participants, within any stratum of observed LDL-C, risk of CAD was higher among FH mutation carriers than noncarriers. Compared with a reference group with LDL-C <130 mg/dl and no mutation, participants with LDL cholesterol >190 mg/dl and no FH mutation had a 6-fold higher risk for CAD (odds ratio: 6.0; 95% confidence interval: 5.2 to 6.9), whereas those with both LDL-C >190 mg/dl and an FH mutation demonstrated a 22-fold increased risk (odds ratio: 22.3; 95% confidence interval: 10.7 to 53.2). Authors conclude that FH mutation carriers had higher cumulative exposure to LDL-C than noncarrier.¹⁷

1.2 Endothelial function and subclinical atherosclerosis

Endothelial dysfunction is the earliest stage of the atherosclerotic process and a trigger of CV events.¹⁸ FH is associated with early development of endothelial dysfunction.¹⁹ Endothelial homeostasis is a complex mechanism, and its alteration triggers the processes that lead to development of atherothrombosis. In normal condition, the vascular endothelium can maintain the homeostatic balance through regulation of inflammatory equilibrium, tight junctional barriers, hemodynamic stability as well as optimally balanced thrombotic and fibrinolytic pathways. More

in detail, under normal conditions endothelial cells (ECs) could be considered as a real “organ” with its own defined structure, capable of guaranteeing vascular homeostasis through several functions.²⁰

To guarantee vascular homeostasis, the endothelium first needs to maintain intact its structure. Several molecules are involved in this process. The main is vascular endothelial-cadherin (VE-cadherin, CD144) that is a component of endothelial cell-to-cell adherent junctions and promotes an optimal organization of the ECs cytoskeleton.²¹

The endothelium is involved in immune response regulation, allowing leucocyte migration into extravascular spaces to defend against infections and promoting tissue repair.²² Furthermore, ECs show on their surface adhesion molecules (E-selectin, P-selectin, L-selectin) and their expression is upregulated by proinflammatory cytokines such as interleukin-1 α (IL-1 α), IL-1 β or tumour necrosis factor- α (TNF- α). Intercellular adhesion molecule-1 (ICAM-1, CD54), vascular cell adhesion molecule-1 (VCAM-1, CD106) and integrins are able to regulate binding between ECs and leucocytes.²³ Endothelium play a key role in regulating thrombosis and the activation of coagulation cascade. However, coagulation is a very complex process that involves many actors, among which the most important are platelets and ECs themselves.²⁰

To prevent abnormal blood clots formation the ECs balance vascular tone producing several factors involved in dilatation of muscular arteries; among these, the most important are nitric oxide (NO) and Prostaglandin I₂(PGI₂) which combines both antiaggregatory and vasodilator effect.²⁴

On this hand, ECs show on their surface a large concentration of molecules involved in the activation of anticoagulant pathways: heparan sulphate (HS) promotes the anticoagulant effect of antithrombin III (ATIII), while thrombomodulin (TM) stimulates protein C and protein S function.²⁵ The endothelium can also express plasminogen activators such as tissue-type plasminogen activator (tPA) and urokinase plasminogen activator (uPA) that enhance fibrinolytic processes.^{26, 27} Moreover, ECs can also produce adhesion molecules for platelets, such as von Willebrand Factor (vWF), P-selectin,

and fibrinogen, which can be exposed on ECs surface when they are activated by IL-1 β and TNF- α ²⁵. In turn platelets produce vascular endothelial growth factor (VEGF), which stimulates the production of tissue factor (TF) from ECs, enhancing the activation of coagulation cascade.²⁸ The shear stress is also an important determinant in endothelial function.²⁹ Mechanisms responsible of endothelial homeostasis are summarized in *Figure 2*.

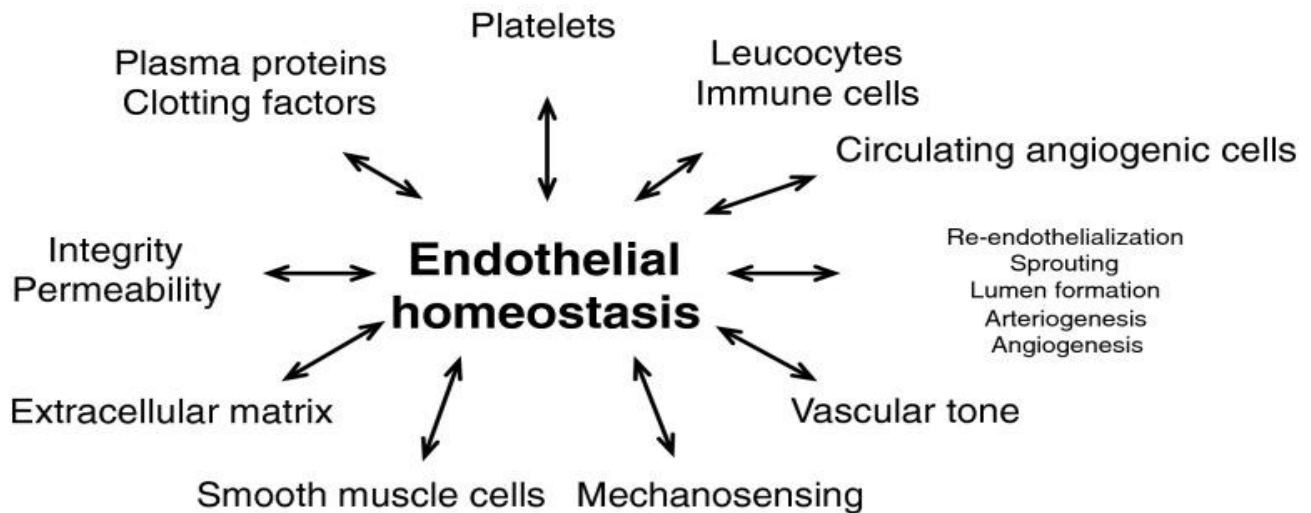


*Figure 2: Key aspects of endothelial homeostasis*³⁰

LDL-C may affect endothelial function mainly because of alterations in NO synthesis, mainly through weakening of endothelial nitric oxide synthase (eNOS).³⁰ Impaired NO synthesis in hypercholesterolemia has been linked to increased plasma concentrations of the endogenous NOS inhibitor ADMA, which have frequently, but not consistently, been observed in patients with hypercholesterolemia.^{31, 32} There is conflicting evidence available regarding the impact of hypercholesterolemia on eNOS expression. Although, some investigators report that expression of eNOS is increased by native or LDL-C,³³ others suggest that expression may be downregulated by oxidized³⁴ or native LDL >160 mg/dL.³⁵ Down-regulation of eNOS expression by native LDL could be prevented by simvastatin through a post-transcriptional mechanism. The effect of LDL-C on gene expression may strongly depend on the stage of disease.³⁶ The load of oxidative stress and isoprostane excretion appears to increase with the stage of atherosclerotic disease.³⁶

The assessment of endothelial dysfunction in humans can be performed through several invasive and not invasive methods. Among these, non-invasive brachial artery assessment of flow-mediated dilation (FMD) is a largely used sensitive and cost-effective technique for assessment of endothelial function.^{37,38} FMD has been introduced for clinical purposes about 15 years ago.³⁹ The FMD is based on the evaluation of the brachial artery diameter percentage change after the deflation of the arm cuff. Several scientific evidence that FMD could represent a reliable method for predicting pre-clinical cardiovascular risk.^{40,41} It consists in the measurement of changes in brachial artery diameter as a response to shear stress. To induce this response, a pneumatic cuff placed on the forearm is inflated up to supra-systolic pressure for 5 minutes. When the cuff is deflated, the increased flow enhances the shear stress on arterial wall which stimulates the local production of NO, causing artery dilatation.⁴²

Endothelial dysfunction is also linked to arterial stiffness. Indeed, arterial stiffening causes greater exposure of the endothelium to hemodynamic load which has been speculated to augment endothelial dysfunction via reducing NO bioavailability and increasing oxidative stress.^{29,33}

Recognizing endothelial dysfunction could bring physicians to an early identification of high-risk patients, giving a more comprehensive assessment of CV risk contributing to better evaluate the best clinical and therapeutic strategy in CV disease. Obviously, despite being a not invasive and not expensive method, it has been observed that in the same study population there can large variations of FMD mean values,⁴³ so more effort is needed in order to provide a standard protocol for the procedure.

1.3 Lipid lowering therapies: from statins to Proprotein convertase subtilisin/kexin type 9 (PCSK9) inhibitors.

Several studies consistently showed that increased levels of LDL-C represent the main causative factor for atherosclerosis development, prevalence of subclinical atherosclerosis and a more rapid

atherosclerosis progression. This leads to a significantly higher CV risk in patients with high LDL-C levels and related oxidative stress.⁴ LDL particle concentration can be lowered by reductions in saturated fat consumption and caloric intake, as well as by multiple classes of cholesterol lowering therapies.^{4, 44, 45} Statins, or inhibitors of 3-hydroxy-3-methyl-glutaryl-coenzyme A reductase, represent the most extensively studied therapies for lowering LDL and ASCVD events.^{4, 46} For every 38.6 mg/dl (1 mmol/l) reduction in LDL-C, ASCVD events are reduced by 21% after 1 year of treatment with moderate- or high-intensity statins.^{4, 45} The amount of ASCVD risk reduction with statin therapy is directly related to the amount of LDL-C lowering expressed as absolute decrease from baseline.

The advent of statin therapy in the 1990s enabled an unprecedented reduction in CV risk and these drugs should be considered one of the major advances in contemporary medicine. However, despite the proven efficacy of these drugs, the therapeutic goal is not always achieved. This problem is further burdened by patients' poor adherence to statin therapy due to muscle-related adverse effects. The clinical consequences of under-treatment are particularly severe for patients at high and very high CV risk, particularly those with FH.⁴⁵

Following the introduction of ezetimibe had modest effects on LDL-C reduction and clinical outcomes in high- and very high-risk patients.⁴⁷⁻⁴⁹ Further development and use of PCSK9 inhibitors (PCSK9i) has led to even more promising new results in the reduction of LDL-C levels, and CV events. Specifically, RCTs have demonstrated that statin therapy combined with either ezetimibe or PCSK9i reduces ASCVD events in high-risk populations.⁴⁷⁻⁴⁹

The 2 currently available antibodies (alirocumab, evolocumab) against PCSK9 are fully human IgG subtypes that bind with an approximate 1:1 stoichiometry to circulating PCSK9 and exclude its binding to the LDLR, thus creating a PCSK9-deficiency state that results in tremendous accumulation of LDLR on the membrane of hepatocytes, accelerated clearance of LDL particles, and large decreases in plasma LDL-C levels⁵⁰ (*Figure 3*).

The subcutaneous injection of 75 to 150 mg of alirocumab or of 140 to 420 mg of evolocumab introduces a vast excess (over 100 to 1, relative to the target) of antibodies that within just a few hours of administration capture all the circulating PCSK9 and will capture all the newly secreted PCSK9 for the following several days.⁵⁰

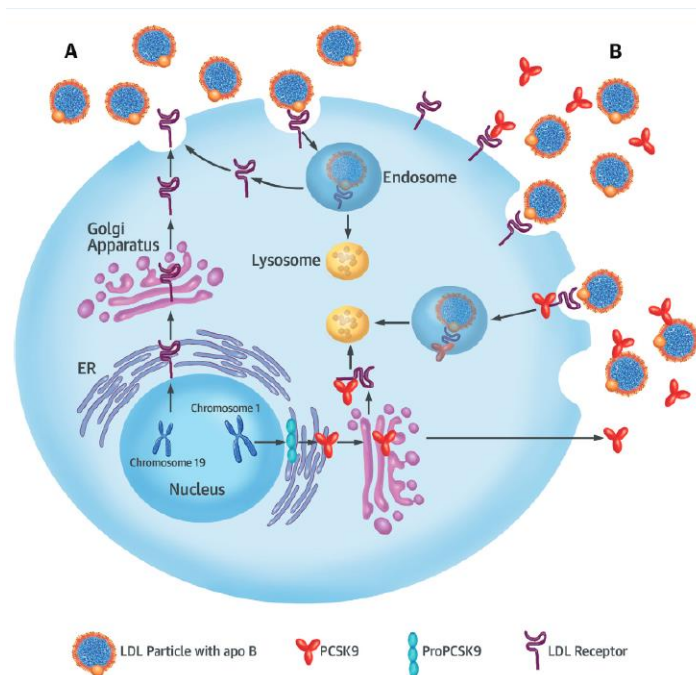


Figure 3: pharmacodynamic of PCSK 9 inhibitors⁵⁰

PCSK9i have proven to be an effective therapeutic approach for the treatment of hypercholesterolemia, and in particular FH⁵¹ in which combination of high intensity statin and ezetimibe often was not enough to reach LDL-C goal.

PCSK9i demonstrated efficacy in LDL-C reduction (median reduction about 50%), in prevention from CV events and in atherosclerotic regression⁵²⁻⁵⁴ but no evidence is available on effect on LDL subfractions. Small dense LDL (sd-LDL) are considered an emerging risk factor for CV disease due to a greater atherogenic potential and are important markers for predicting CV risk.⁵⁵

1.4 Potential pleiotropic effects of PCSK9 inhibitors

It is well known that statins produce pleiotropic effects improving endothelial function and reducing oxidative stress. The reduction of CV events attained with statins in some clinical trials, like the

JUPITER trial⁵⁶ has been indeed greater than that expected solely from LDL-C reduction. Since the damaging effect of LDL-C on the CV system is concentration-dependent, the reduction of ischaemic cardiovascular events produced by PCSK9i when added to statins has been ascribed primarily to their further, strong LDL-C-lowering action. In a recent meta-analysis of trials with lipid-lowering interventions including more than 300,000 patients, the relative risk reduction of major vascular events associated with PCSK9i use was higher, even if not significantly, than that observed with statins for the same LDL-C reduction (OR, 0.49 (95% CI, 0.34–0.71) vs. 0.61 (95% CI, 0.58–0.65)).⁵⁷ Although, effects on HDL and the ability to reduce lipoprotein (a) Lp(a) of PCSK9i were considered also potential pleiotropic effects on other lipids classes or independent from lipid metabolism could also be considered but few data are available.

Current evidence has shown that plasma PCSK9 levels are associated with future risk of CV events, and the inhibition of PCSK9 to lower LDL-C levels reduces the risk.⁵⁸ However, recent studies found that the PCSK9 levels could also predict CV events even in those patients with well-controlled LDL-C levels, suggesting that the effects of PCSK9 on CV systems might be mediated by LDL-independent mechanisms.^{58, 59}

PCSK9 plays a significant role in vascular remodelling and atherothrombosis.¹² PCSK9 is produced by vascular cells such as vascular smooth muscle cells (VSMC), EC and, at lower level, by macrophages.¹² PCSK9 acts in a paracrine manner, downregulating LDLR expression on the cell surface of macrophages¹² and avoiding the formation of foam cells, enhancing atherosclerosis progression. Moreover, the inflammatory milieu in vascular tissue potentiates the crosstalk between PCSK9 and oxidated LDL receptor (LOX-1), in which PCSK9 stimulates LOX-1 and LOX-1 stimulates PCSK9.¹² Both EC and VSMC show PCSK9 protein expression is higher under low blood flow than high blood flow.¹² Therefore, a negative correlation exists between PCSK9 vascular expression levels and blood flow. These findings support the concept that, in addition to its well-established action on LDLR modulation in hepatocytes, PCSK9 can also exert direct effects on

atherogenesis in the absence of systemic lipid changes, engaging with other receptors or proteins involved in atherosclerosis pathogenesis.¹²

Moreover, the relationship between plasma PCSK9 levels and platelet reactivity has been investigated in the past few years, whereas the direct effects of PCSK9 on platelet activation and the underlying mechanisms remain unclear. Camera et al.⁶⁰ showed that human recombinant PCSK9 (5 µg/mL) promoted epinephrine-induced platelet aggregation, and knockout (KO) mice for PCSK9 mice showed a reduction of FeCl₃ injury-induced carotid artery thrombosis.⁵⁸⁻⁶⁰

PCSK9 in plasma directly enhances platelet activation and in vivo thrombosis by binding to platelet CD36 and thus activating the downstream signalling pathways.⁵⁹ PCSK9, through the CD36 and LOX-1 downstream activation of Src-kinase and mitogen-activated protein kinase (MAPK)-extracellular signal-regulated kinase 5 and c-Jun N-terminal kinase pathways, leads to increased cyclooxygenase-1 (COX-1) activity and, consequently, thromboxane A₂ synthesis.⁵⁹ PCSK9 inhibitors or aspirin abolish the enhancing effects of PCSK9, supporting that the use of aspirin in patients with high plasma PCSK9 levels in addition to PCSK9 inhibitors are useful to prevent thrombotic complications.⁵⁹

1.5 Project Aim:

The aim of the present project is to evaluate effects of PCSK9i on lipid profile, lipid sub-fractions (sd-LDL and Lp(a)), subclinical atherosclerosis (assessed by FMD and carotid stiffness) and to explore potential pleiotropic effects of PCSK9i using an untargeted multi-omic approach before and at different time points, following treatment with the PCSK9i (evolocumab).

2. Methods:

From December 2017 to December 2018, within the framework of LIPIGEN, a national project on familial dyslipidemia,⁶¹ consecutive patients attending the lipid clinic of the Department of Clinical

Medicine and Surgery, Federico II University Hospital with very high levels of LDL-C (above the 95th percentile when compared with a sex- and age-matched general population), normal triglyceride levels and presumed autosomal dominant transmission of hypercholesterolemia (DUTCH Lipid Clinic Network score > 6) in the family were screened for inclusion in the present study.⁶²

The major inclusion criterion was the eligibility of patients to start a treatment with PCSK-9 according to ESC/EAS guidelines.⁴ Exclusion criteria were: age < 18 years, inability to understand or sign the informed consent, high level of transaminases (>3x upper normal limit), hypertriglyceridemia (>150 mg/dl), end-stage renal disease (filtration rate < 30 ml/min/mq), current malignant disease or a diagnosis of malignancy in the 2 years prior to the first visit, previous exposure to PCSK9i, presence of hypercholesterolemia secondary to other causes (hypothyroidism, hormone therapies, corticosteroids etc.). Patients with a clinical picture or family history of familial combined hyperlipidemia were excluded⁶³. Patients enrolled in the study continued the ongoing lipid lowering therapy and added PCSK9i (evolocumab 140 mg subcutaneous injection every 14 days).

2.1 Study protocol

After informed consent, a detailed medical history was recorded for each patient. Data about age, gender, previous and/or current medical conditions, current and past lipid lowering therapy, vascular risk factors were collected.

Height was measured to the nearest 0.1 cm. Body weight was assessed by using an electronic beam scale with digital readout to the nearest 0.1 kg after emptying the bladder and with the subjects standing barefoot and wearing light indoor clothing. Body mass index (BMI) was calculated as body weight/(height²). Clinical diagnosis of FH was achieved using Dutch Lipid Clinic Network

Score and genetic testing was performed to assess major causative mutations, including *LDLR*, *APOB* and *PCSK9* genes as previously described.^{64, 65}

Study protocol flow-chart is summarized in *Figure 4*

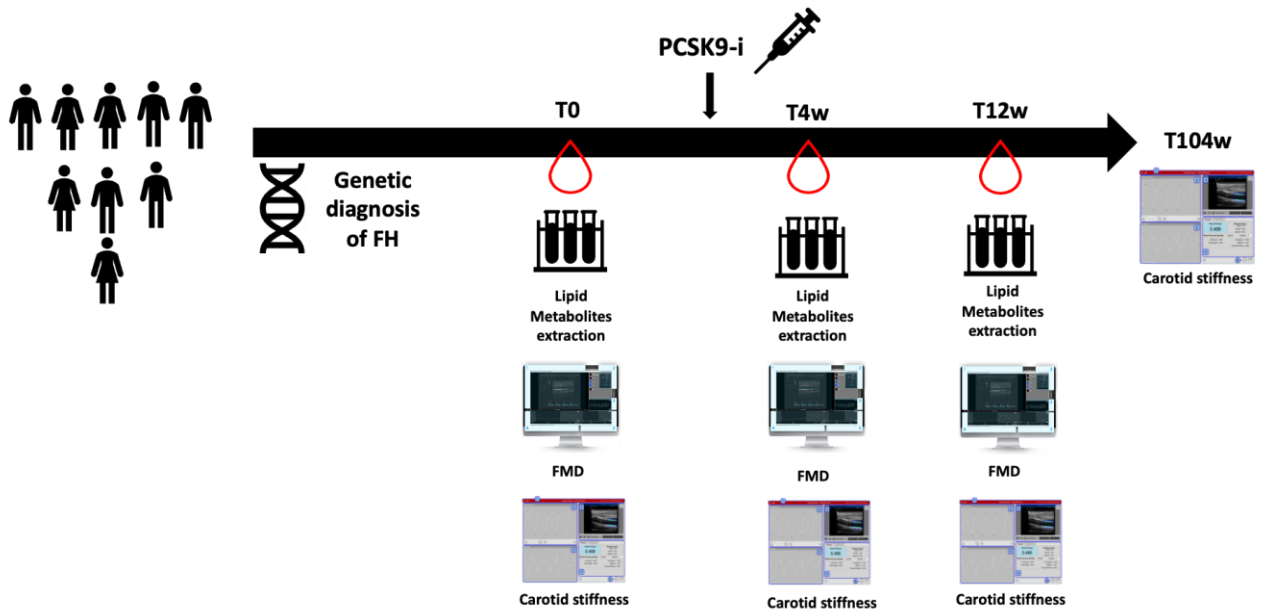


Figure 4: Study flow-chart

2.2 Blood laboratory parameters

The following blood values were evaluated at baseline (before starting PCSK9 inhibitor) and 12 weeks (T12w) after treatment with evolocumab: total cholesterol (TC), triglycerides (TGL), HDL cholesterol (HDL-C), LDL-C, small-dense LDL (sd-LDL), creatininemia, AST, ALT, CPK, glycaemia.

LDL particles separation was performed by electrophoretic Lipoprint System (Quantimetrix Inc., Redondo Beach, CA). The proportion of sd-LDL particles (subfractions 3–7) to the whole LDL area (subfractions 1–7) was also calculated in our sample and expressed as LDL score, with higher score values representing a higher sd-LDL particles content.⁶⁶ In addition, mean LDL particle diameter was calculated on the basis of the different areas under the curve of the 7 LDL species with different electrophoretic mobility.⁶⁷

Urine samples were collected in the morning and stored in polypropylene tubes at -80°C .

Oxidative stress was evaluated by assessing urinary 11-dehydro-thromboxane (11-TXB₂) and 8-isoprostaglandin-2 α (8-iso-PGF₂ α) using electrospray ionization tandem mass spectrometry.

2.3 Untargeted Lipidomic Analysis

2.3.1 Lipid Extraction

Frozen plasma samples were thawed in ice, and 100 μL aliquots were transferred into 10 mL borosilicate tubes. Lipids were extracted by using a slightly modified Bligh and Dyer system 13671378. Briefly, 3 mL of chloroform:methanol 2:1 (v:v) containing 20 mg/L butylhydroxytoluene (BHT) was added; samples were vortexed for 10 s and sonicated in ice for 15 min in an ultrasonic bath (Falc, LabService, Milan, Italy). One milliliter of deionized water was added; samples were vortexed for 10 s and centrifuged at 3500 rpm for 10 min at 4°C to promote phase separation. The organic phase was collected, and the aqueous phase was re-extracted by adding 2 mL of chloroform 20 mg/L BHT. The pooled organic phase was dried in a Speedvac and re-suspended in 300 μL methanol–chloroform 9:1 (v:v). Quality control samples were obtained by pooling 50 μL volumes of each sample.

2.3.2 UHPLC-ESI-Q-TOF–MS Analysis

Lipids were injected on an Agilent 1290 Infinity UHPLC (Agilent Technologies, Santa Clara, CA, USA) connected with an Agilent 6550 iFunnel Q-TOF mass spectrometer equipped with a Dual-Jet ESI source (Agilent, Milan, Italy). Lipids were separated under reverse-phase conditions on a ZORBAX Eclipse Plus C18 Rapid Resolution HD column (2.1 mm \times 150 mm, 1.8 μm ; purchased by Agilent, Milan, Italy) and eluted at 0.3 mL/min. Mobile phase A was acetonitrile–water 50:50 (10 mM ammonium formate, 0.1% formic acid), and B was acetonitrile–water–isopropanol 10:2:88 (10 mM ammonium formate, 0.1% formic acid). The linear gradient, starting at 65%A:35%B, reached 95%B in 20 min and 100%B in 5 min; final conditions were kept for 2.5 min to ensure

complete elution of non-polar lipids. Initial conditions were reached in 0.5 min and maintained for 10 min to ensure a complete column re-equilibration.

Full-scan analysis over m/z 100–1200 in positive ion mode and over m/z 50–1200 in negative was carried out at a scan rate of 1.50 spectra/s. To avoid detector saturation, 0.2 μL of lipid extract was injected in positive ion mode and 2 μL in negative ion mode. Additional mass spectrometry settings were the following: gas temp, 230 °C; gas flow, 12 L/min; nebulizer, 35 psig; sheath gas temp, 350 °C; sheath gas flow, 12 mL/min; V cap, 3500 V for positive, 4000 V for negative; Nozzle voltage, 1000 V; fragmentor, 150 V; skimmer 1, 65 V; octopole RF peak, 750 V. MS/MS studies were carried out under the same experimental conditions using a collision energy of 30 V.

Samples were randomized prior to injection. Quality controls (QCs) were injected six times prior to analysis, every 8 samples, and at the end of the acquisition to address the instrumentation stability.

Data were acquired with MassHunter software (version B.07.00; Agilent, Milan, Italy).

2.3.3 Lipid Annotation and Data Analysis

Lipids were annotated according to their m/z acquired in high-resolution mode; database search (Lipid Maps (www.lipidmaps.org (accessed on 10 October 2021)), Human Metabolome Database (www.hmdb.ca (accessed on 10 October 2021)), CEU Mass Mediator (www.ceumass.eps.uspceu.es (accessed on 10 October 2021)), and Mass Bank (www.massbank.jp, accessed on 10 October 2021)); and after MS/MS experiments in positive and negative ions. Lipids were denoted by head group, total fatty acyl carbon atoms and unsaturation content (e.g., PC 34:1). For ether/vinyl ether species, both species are reported when it was not possible to annotate the correct form (e.g., PC (O-36:3)/(P-36:2)).

Raw data were processed by MZmine 2.3 (www.mzmine.github.io (accessed on 10 October 2021)).

In positive ion mode, phosphatidylcholine (PC) and lyso-PC (LPC), sphingomyelin (SM), diacylglycerol (DAG), triacylglycerol (TG) and cholesteryl ester (CE) were detected and annotated.

In negative ion mode phosphatidylethanolamine (PE) and lyso-PE (LPE), phosphatidylinositol (PI) and lyso-PI (LPI), phosphatidylserine (PS), ceramide (CER), glucosyl/galactosyl-ceramide (HEX-CER), lactosyl-ceramide (LAC-CER) and 3-O-sulfogalactosylceramide (S-HEX-CER) were detected and annotated. Residual missing values in the data matrix were imputed using Random Forest package in R (www.r-project.org (accessed on 10 October 2021)). Data were normalized by Loess-global regression using the Normalyzer tool 24766612. Multivariate statistics was carried out by MetaboAnalyst 4.0 software (www.metaboanalyst.ca (accessed on 10 October 2021)). Pareto was used as the scaling factor, to make variables comparable to each other. Analysis of Variance (ANOVA) with False Discovery Rate multiple testing correction (FDR) was applied to detect features significantly different after treatment, setting a p-value threshold of 0.05.

For each lipid class, we calculated the Unsaturation Index (UI), an estimate of the average number of unsaturations, using the formula: $UI_y = (\sum (\% \text{ area lipid}_x \times \text{number of double bonds lipid}_x))/100$, where lipid_x represents each single molecular species belonging to the y lipid class, and the Average Chain Length (ACL), an estimate of the average length of acyl chains, using the formula: $ACL_y = (\sum (\% \text{ area lipid}_x \times \text{total number of acyl chains—carbon atoms of lipid}_x))/100$.

2.4 Untargeted Metabolomic Analysis

2.4.1 Untargeted LC-MS Metabolite Profiles

From each patient and at each time point of the study, blood was collected in EDTA and immediately centrifuged at 600× g for 15 min to obtain plasma samples that were aliquoted and stored at −80 °C until analyzed. All the samples were thawed on ice before analysis, and 100 μL aliquots of each of them were added to a reference standard solution, i.e., acetonitrile:methanol (50:50 v/v) solution containing reserpine, 3-nitro-L-tyrosine-13C₉ (3-nitro-tyr-13C₉), L-4-tyrosine-13C₉ (L-4-tyr-13C₉), and trimethylamine-N-oxide (TMAO-d₉) at a final concentration of 4 ng/μL; rivastigmine, acetylsalicylic acid-d₄ (ASA-d₄), prostaglandin F₂α-d₄ (PGF₂α-d₄), 8-hydroxy-2-deoxyguanosine-15N₅ (8-OHdG-15N₅), and 11-dehydro-thromboxane B₂-d₄ (11-DH-TXB₂-d₄) at

final a final concentration of 2 ng/ μ L; 12-hydroxyeicosatetraenoic acid-d₈ (12-HETE-d₈) 1 ng/ μ L and methionine C13 0.8 ng/ μ L. Protein precipitation was achieved by adding to each sample 300 μ L of a precooled acetonitrile:methanol (50:50 v/v) solution; the mixture was vortexed for 10 s at room temperature and stored for 20 min at -20 °C. Samples were then centrifuged at 12,000 RCF (relative centrifugal force) at 4 °C for 20 min and the supernatant was transferred into vials for metabolomics analysis. Ultra-high-performance liquid chromatography analysis was performed by an Agilent 1290 Infinity UHPLC system (Agilent Technologies, Santa Clara, CA, USA) coupled to a quadrupole time-of-flight mass spectrometry detector (Agilent 6550 iFunnel Q-TOF) equipped with a Dual-Jet ESI source (Agilent, Milan, Italy). Two-microliter samples were injected into a ZORBAX Eclipse Plus C18 Rapid Resolution HD Agilent column (2.1×150 mm, 1.8 μ m) through an autosampler at 4 °C. The column temperature was set at 60 °C and the flow rate was 0.5 mL/min. Metabolite detection was programmed in both positive and negative ion modes. Mobile phases for both analyses were: water:acetonitrile (95:5 v/v) with 0.1% formic acid (A) and acetonitrile:water (90:10 v/v) with 0.1% formic acid (B). The UHPLC gradient was programmed as follows: 1 min with 100% A, 2–8 min with 100–20% A, 8–11.5 min with 20–0% A, 11.5–12.5 min with 0% A, and 12.5–13.5 min with 0–100% A. Initial conditions were reached in 1 min and maintained for 10 min to ensure a complete column re-equilibration. The detector operated in full-scan mode, acquiring mass spectra over the m/z range of 50–1100 Da, with a scan rate of 1.50 spectra/s. The following additional mass spectrometry setting conditions were employed: gas temp., 250 °C; gas flow, 12 L/min; nebulizer, 45 psig; sheath gas temp., 370 °C; sheath gas flow, 11 mL/min; V cap, 3000 V for positive, 4000 V for negative; nozzle voltage, 1000 V; fragmentor, 150 V; skimmer 1, 65 V; octopole RF peak, 750 V. Samples were analyzed in separate runs (positive and negative ionization modes), in a randomized order. Quality control (QC) samples, obtained by mixing 50 μ L of each plasma sample subsequently enriched with the reference standard solution, were used to improve the equilibrium at the beginning of analysis ($n = 8$) and at regular time intervals (every eight injections) to monitor system stability and performance. The QC samples

mixed with reference standard solution were prepared together with samples according to the same protocol. MS/MS analysis were performed on the QC samples only for significant compounds, using the same chromatographic separation and ionization conditions reported above. Compounds were targeted using their m/z value (narrow 1.3 Da) and RT (Δ RT 0.9 min), and fragmentation was achieved using two fixed collision energies, 10 and 40 eV. The reference ions, continuously infused into the system, were m/z 121.050873 and m/z 922.009798 in positive ion mode and m/z 119.036320 and m/z 966.000725 in negative ion mode, respectively.

2.4.2 LC-MS Data Collection

A preliminary quality check of the data collected by LC-MS was performed by MassHunter Qualitative Analysis software (Agilent Technologies). The untargeted metabolomics raw data were processed by MassHunter Profinder software (Agilent Technologies) using the 'Batch Recursive Feature Extraction' algorithm that allows for cleaning from background noise and unrelated ions. The parameters used for mass extraction were: 500 counts for the peak filter; charge state limited to 2; permitted ion species for positive ion mode: +H, +Na, and +K, and -H, +Cl, and +CH₃COO for negative ion mode; and neutral loss of water for both ion modes. To further reduce the acquired data size and complexity, a manual feature evaluation was performed by removing redundant and nonspecific information. This resulted in a dataset comprising a total of 1270 features (625 for the positive ion mode and 645 for the negative ion mode).

2.4.3 Metabolites Identification

Identification of the metabolites was performed by searching their measured accurate m/z values (10 ppm mass error window) against online available databases such as Metlin (<http://metlin.scripps.edu>) (accessed on 15 July 2021), Kyoto Encyclopedia of Genes and Genomes (<http://www.kegg.jp/kegg>) (accessed on 15 July 2021), Human Metabolome Database (<http://www.hmdb.ca>) (accessed on 15 July 2021), and Personal Compound Database and Library (Agilent Technologies). The results were subsequently verified by comparing their acquired

MS/MS spectra with those available on different databases. Annotation or identification was determined following the official classification defined by the Metabolomics Standard Initiative.

2.5. Subclinical atherosclerosis markers

2.5.1 Brachial artery flow-mediated dilatation (FMD) with post-ischemic hyperemia (PIH)

Patients were asked to abstain from alcohol, tobacco and caffeine on the day of FMD assessment. All study procedures were performed in a temperature-controlled room (23°C), with the study subject in a resting position before measurements began. Assessment of FMD was performed after ≥ 10 minutes of rest in supine position (a small head pillow was accepted) and each measurement was performed on the day of hospitalization and repeated at each time-point (before starting antiviral therapy, at the end of therapy and three months after the end of the therapy).

Brachial artery FMD and PIH were evaluated in each patient at each time-point (before starting antiviral therapy, at the end of therapy and 12 weeks after the end of the therapy) by the same operator in blinded conditions as to disease activity. FMD and PIH were measured by ultrasound imaging, as described in the guidelines of the International Brachial Artery Reactivity Task Force.³⁷

After 12-hour fasting and avoiding smoking, in each patient we evaluated FMD and PIH of the brachial artery according to a standardized ultrasound protocol using an automatic edge detection software (Cardiovascular Suite®, FMD studio, QUIPU Srl, Pisa, Italy). The examination consisted in measuring brachial artery diameter (BAD) at rest and after reactive hyperemia induced by ischemia of the forearm. The measurement was made on a B-mode section of the artery, which was imaged above the antecubital fossa in the longitudinal plane by using a linear ultrasound vascular transducer with a frequency of 10 MHz (Esaote®, MyLab 25 Gold, Pisa, Italy). Baseline brachial artery diameter and the flow velocity were recorded for 60 seconds. The blood pressure cuff was placed on the forearm 4-5 cm behind elbow joint line and inflated up to 70 mmHg above the systolic blood pressure to induce a transitory ischemia for 300 seconds. After cuff release, FMD was calculated as (Max

diameter post-ischemic – Basal diameter)/ Basal diameter x 100 and expressed as percent of brachial artery diameter increase compared with baseline value. The PIH was defined by share rate area under the curve during reactive hyperemia after cuff release. The reactive hyperemia index (RHI) was calculated as (average flow velocity after cuff deflation/flow velocity measured at the baseline) and defined as low when < 1.67 .⁶⁸ The duration of the overall exam was about 10-15 minutes. The reproducibility of this scanning protocol was evaluated on a representative sample of 5 subjects randomly selected from the study population within 1 week from the first examination.

2.5.2 Carotid stiffness and distensibility

Patients were asked to abstain from alcohol, tobacco and caffeine for at least 12 hours on the day of examination. All study procedures were performed in a temperature-controlled room (23°C), after ≥ 10 minutes of rest in supine position. Carotid stiffness was evaluated in each patient before starting PCSK-9 inhibitor (T0) and repeated after 12 weeks of treatment (T12w) by the same operator blinded for ongoing treatment and cholesterol levels. To validate results on the long-term, carotid stiffness parameters were evaluated also after 104 weeks of treatment (T104w)

Common carotid artery scans (25 frames/s) were obtained by high-resolution ultrasound with a 10 MHz linear array transducer (MyLab25; ESAOTE, Florence, Italy) by a trained operator.

Longitudinal scans were acquired from each common carotid artery (1 cm proximal to the carotid bulb in a region 1-cm wide and free of plaques) and automatically analyzed with Carotid Studio (Cardiovascular Suite®, Carotid studio, QUIPU Srl, Pisa, Italy), a well validated system based on contour tracking algorithm.⁶⁹ Arterial interfaces were automatically detected, with estimation of instantaneous mean diameter as the distance between far and near media–adventitia interfaces. The following parameters were obtained: carotid distension (ΔD), that is the stroke change in diameter, calculated as the difference between the systolic and diastolic diameter values; carotid distensibility coefficient = $\Delta A / (A * \Delta P)$, where A represents the diastolic lumen area, evaluated from the diameter

values (assuming the cross-section of the artery to be circular), ΔA represents the stroke change in lumen area, ΔP the local pulse pressure obtained by tonometry. Carotid stiffness was calculated according to the Moens–Korteweg equation.⁷⁰ In particular, carotid distensibility was converted into carotid stiffness by using the equation: $PWV = ((\Delta P * A)/(\Delta A * r))(1/2)$ where r is the blood density. This formula allows carotid stiffness to be obtained as $\text{carotid stiffness} = (r * \text{carotid distensibility})^{-1/2}$, expressed in m/s. The reproducibility of this scanning protocol was evaluated on a representative sample of 5 subjects randomly selected from the study population within 1 week from the first examination and the r value resulted = 0.91. Carotid distensibility was defined as low if $< 15 \text{ kPa}^{-1} \times 10^{-3}$.⁷¹

2.6 Statistical analysis

Statistical analysis was performed with the IBM SPSS 22 system (SPSS Inc., Chicago, IL, USA). Continuous data were expressed as mean \pm standard deviation (SD) or as median value with interquartile range (IQR). The t-test was performed to compare continuous variables for paired samples and for independent samples. In case of values with a skewed non-Gaussian distribution, Mann-Whitney U test was used to compare means. The χ^2 test or Fisher's exact test were used to compare categorical variables. Relationships between continuous variables were examined using simple regressions Spearman's correlation (ρ) for non-parametric variables. All results were expressed as 2-tailed values, p values < 0.05 being statistically significant. To evaluate potential sources of heterogeneity, a sensitivity analysis was performed stratifying patients according to major clinical and demographic characteristics and according to genotype of *LDLR*, *APOB* and *PCSK9* genes. To adjust for potential confounders and to make predictions, linear regression analyses (stepwise method) were implemented with changes in carotid stiffness as dependent variable and age, gender, BMI, cardiovascular events, hypertension, diabetes and changes in LDL score as independent variables.

For metabolomics analyses, Compounds with more than 4 missing values were removed. The remaining missing data were imputed exploiting the 'rfImpute' function, embedded in the 'randomForest' R package.⁷² The QC signal correction and a global normalization were sequentially applied by the 'QC-RLSC' strategy and the LOESS normalization, respectively.⁷³ Differential analyses, evaluating the effect of PCSK9 over time, were performed by the 'limma' R/Bioconductor package.⁷⁴ The Benjamini-Hochberg procedure was used to control for the false discovery rate (FDR). A compound was deemed significant if the FDR adjusted p-value was < 0.05 .

2.7 Sample size

As to sample size, with a pre-defined reduction in carotid stiffness from baseline values to $T1 \geq 25\%$, 22 subjects were needed to obtain an 80% power and a 5% α error.

Furthermore, as to sample size, with a pre-defined increase in FMD from baseline values to $T12w \geq 50\%$, 16 subjects were needed to achieve an 80% power with a 5% α error. Also considering a drop-out risk, we aimed at enrolling 25 subjects in the present study. For untargeted multi-omic analyses sample size determination is not applicable.

3. Results

3.1 Clinical and demographic

Twenty-five subjects (13 males and 12 females, mean age 51.5 ± 14.5 years) with FH (20 heterozygotes for the mutation of LDLR, 2 compound heterozygotes for 2 different mutations of LDLR, 1 double heterozygote for mutations of LDLR and of PCSK9 and 2 subjects were without major mutation in LDLR, APOB, PCSK9 genes) were enrolled. The mean Dutch Lipid Clinic Network Score was 9.3.

Nineteen patients (76%) were under statin treatment, whereas 6 reported statin intolerance. Among the 19 statin-treated patients, 1 was under simvastatin 40 mg, 3 rosuvastatin 40 mg, 5 rosuvastatin 20 mg, 1 pravastatin 40 mg, 1 fluvastatin 40 mg, 5 atorvastatin 40 mg, 3 atorvastatin 80 mg. Thus, 16 patients were under high intensity-statin treatment (atorvastatin 40 mg or 80 mg; rosuvastatin 20 mg or 40 mg), the other 3 patients being treated with low-intensity statins (pravastatin, fluvastatin and simvastatin) because of intolerance to high intensity-statin. Ezetimibe was present as co-treatment in 16 subjects (68%) and as a stand-alone treatment in the 6 subjects (20%) with statin intolerance, whereas 3 patients (12%) were under statin-alone therapy without ezetimibe because of ezetimibe intolerance. Antiplatelet drugs were used by 9 subjects (36%). None had received a treatment with PCSK-9 inhibitor before study entry. Previous vascular events were reported by 7 subjects (28%), with coronary artery disease being reported in 6 cases and ischemic stroke in 1 case. Patients enrolled in the study reported no adverse events during the entire follow-up. Major baseline clinical and demographic characteristics of the study population are reported in **Table 1**.

Table 1. Clinical and demographic features of subjects with severe hypercholesterolemia starting a treatment with PCSK9 inhibitor.

Variable	Study subjects (n=25)
Age (years)	51.5±14.5
Age > 65 years	4 (16%)
Male gender	13 (52.0%)
Hypertension	12 (48%)
Cardiovascular events	7(28%)
Obesity	13 (52%)
Diabetes	2 (8%)
Smoking habit	2 (8%)
Body Mass Index (BMI) (Kg/m ²)	26 ± 4,8
DUTCH score	9,32 ± 3,64
Without major mutations	2 (8%)
Heterozygotes	20 (80%)
Compound/double heterozygotes	3 (12%)

Alanine aminotransferase (ALT) (IU/L)	24 (IQR:21-26)
Aspartate aminotransferase (AST) (IU/L)	27 (IQR: 21,3- 38,8)
Creatine phosphokinase (IU/L)	110 (IQR: 90-171)
Total Cholesterol(mg/dl)	279,6 ± 69,9
Triglycerides (mg/dl)	107,5 (IQR: 79.3-146,3)
HDL-C (mg/dl)	53 ±12,93
LDL-C (mg/dl)	201±69,50
LDL score	6,6 (IQR:4,65-11,7)
LDL diameter (Å)	268.3 ± 2.99
Use of statins	19(78%)
Statin intolerance	6 (22%)
Use of ezetimibe + statin	16 (66%)
Use of ezetimibe alone	6 (22%)
Use of antiplatelet drugs	9 (36%)

Note. Data are presented as number (%) for dichotomous variables, mean ± standard deviation for continuous variables with a normal distribution and median (interquartile range [IQR]) for non-parametric continuous variables.

3.2 Serum Cholesterol Profile and Lipoprotein Levels after 4- and 12-Week Treatment

As expected, after 4-week treatment with PCSK-9 inhibitor (T4w), all patients showed an improved lipid profile. TC was reduced from 279.6 ± 69.9 mg/dL to 177.3 ± 68.2 mg/dL ($p < 0.001$), LDL from 201.0 ± 69.5 mg/dL to 100.2 ± 70.5 mg/dL ($p < 0.001$), and Lp(a) from 69.3 mg/dL (IQR: 19.8–83.4) to 52.3 mg/dL (IQR: 17.0–80.6) ($p = 0.002$). The % of patients with high-Lp(a) was 56.5% both at baseline and at T4w. LDL-C target was achieved in 14/25 patients (56%), being more frequently found in patients receiving combined treatment statin+PCSK-9 inhibitor (73.7%). LDL diameter changed from 268.3 ± 2.99 Å to 270.4 ± 3.02 Å ($p = 0.003$), an event associated with LDL score reduction from 6.60 (IQR: 4.65–11.7) to 3.0 (IQR: 0.8–7.9) ($p = 0.037$). Correlation between changes in LDL diameter and LDL score was $\rho = -0.770$, $p < 0.001$. TGL (from 107.5 (IQR: 79.3–146.3) mg/dL to 97.0 (IQR: 62.5–119.5) mg/dL ($p = 0.157$)) and HDL (52.5 ± 12.9 mg/dL at T0 vs. 53.2 ± 12.8 mg/dL at T4w ($p = 0.616$)) were not affected by 4-week treatment.

After 12 weeks of treatment with the PCSK-9 inhibitor (T12w), patients reported approximately 34.9% lower levels of TC (from 279.6 ± 69.9 mg/dL to 181.8 ± 64.8 mg/dL, $p < 0.001$) and approximately 48.7% (201.0 ± 69.5 mg/dL to 103.0 ± 58.0 mg/dL, $p < 0.001$) reduction in LDL, with a slight increase in HDL (from 52.5 ± 12.9 mg/dL to 55.0 ± 12.6 mg/dL ($p = 0.065$)). LDL-C target was achieved in 15/25 patients (60%). LDL diameter changed from 268.3 ± 2.99 Å to 270.5 ± 2.40 Å ($p = 0.004$) with LDL score changing from 6.60 (IQR: 4.65–11.7) to 3.7 (IQR: 0.37–4.9) ($p = 0.001$).

The correlation between changes in LDL diameter and LDL score was $\rho = -0.730$, $p < 0.001$. TGL did not significantly change (from 107.5 mg/dL, IQR: 79.3–146.3 mg/dL to 109.0 mg/dL, IQR: 73.5–146.0 mg/dL, $p = 0.607$). In contrast, Lp(a) changed from 69.3 mg/dL (IQR: 19.8–83.4) to 41.7 mg/dL (IQR: 13.5–80.6) ($p = 0.001$). However, the % of patients with high-Lp(a) was only slightly. Median percentage changes in lipid profile are reported in *Figure 5*.

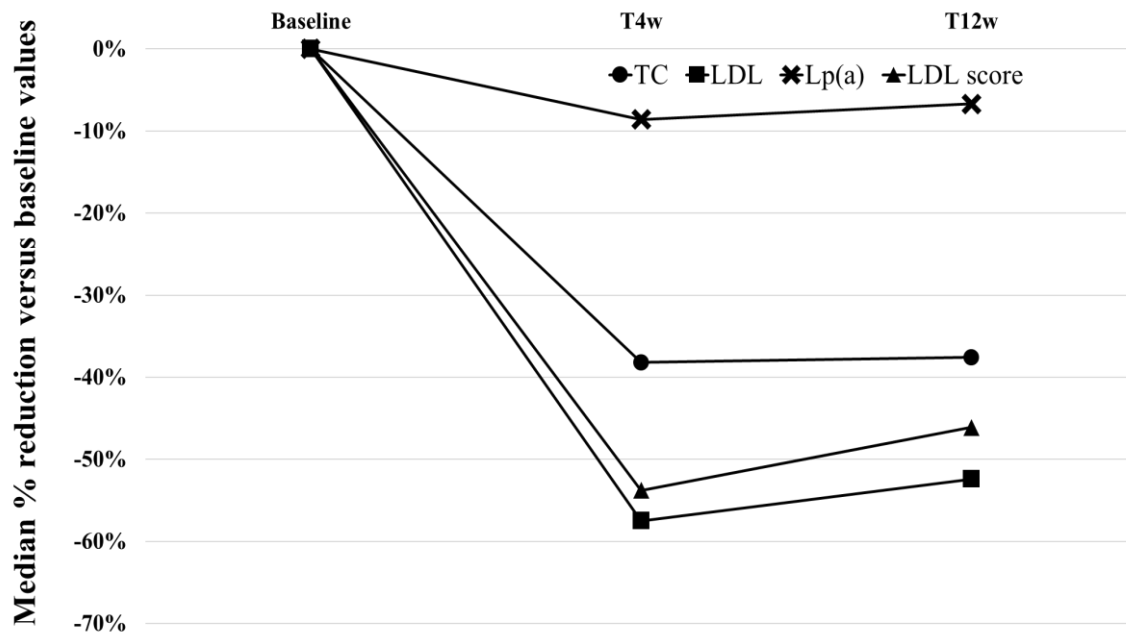


Figure 5: Percent changes in lipid profile and lipoprotein levels during treatment with PCSK-9 inhibitor. Note to Fig. 5: all changes were statistically significant as compared to baseline values.

As showed in **Figure 6**, median cholesterol sub-fraction reduction was more pronounced in patients with LDLR heterozygote mutation or in patients without major mutations as compared to compound heterozygote/double heterozygote ones.

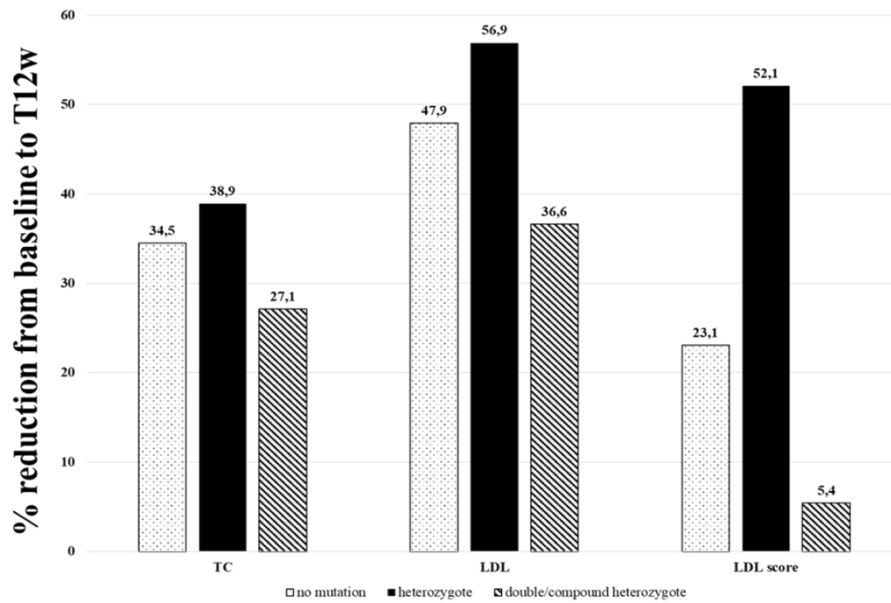


Figure 6: Percent changes in cholesterol profile and lipoprotein levels during treatment with PCSK9 inhibitor stratified according to genotype.

3.3 Effects of PCSK9 Inhibitor on Plasma Lipidome

After the 12-week treatment, 26 lipid features belonging to phosphatidylcholine (PC), sphingomyelin (SM), ceramide (CER), cholesteryl ester (CE), triacylglycerol (TG) and phosphatidylinositol (PI) classes, were significantly reduced from baseline, while 4 species (3 CER and 1 PI) were increased after the treatment (Table 2).

Table 2: Lipid molecular species significantly differing from baseline values according to ANOVA analysis.

Lipid molecular species	Lipid class	Adjusted <i>p</i> -value	Change
PC 34:2 [M+H] +	PC	0.0042255	↓
PC 36:2 [M+H] +	PC	0.0067707	↓

PC 36:4 [M+H] +	PC	0.020646	↓
PC 37:6 [M+H] +	PC	0.0067707	↓
PC 38:4 [M+H] +	PC	0.04987	↓
PC (O-32:0) [M+H] +	PC	0.043201	↓
PC (O-36:3) (P-36:2) [M+H] +	PC	0.011944	↓
PC 34:1 (OH) [M+H] +	PC	0.039059	↓
SM (d33:1) [M+H] +	SM	0.043486	↓
SM (d34:0) [M+H] +	SM	0.00057655	↓
SM (d38:2) [M+H] +	SM	0.011944	↓
SM (d40:2) [M+H] +	SM	0.011944	↓
SM (d42:1) [M+H] +	SM	0.0071241	↓
SM (d42:2) [M+H] +	SM	0.00057655	↓
SM (d42:3) [M+H] +	SM	0.011944	↓
TG 47:3 [M+Na] +	TG	0.017528	↓
TG 51:1 [M+Na] +	TG	0.016612	↓
CE 20:4 [M+H] +	CE	0.041264	↓
CE 18:2 [M+H] +	CE	0.041264	↓
CER (d33:1) [M+HCOONH4]-	CER	0.0071241	↓
CER (d38:1) [M+HCOONH4]-	CER	0.043201	↓
CER (d40:0) [M+HCOONH4]-	CER	0.012228	↓
CER (d42:0) [M+HCOONH4]-	CER	0.016612	↓
CER (d44:0) [M+HCOONH4]-	CER	0.043486	↓
HEX-CER (d42:2) [M+HCOO]-	CER	0.024282	↓

PI 38:5 [M-H]-	PI	0.020376	↓
CER (d43:1) [M+HCOO]-	CER	0.0065246	↑
CER (d44:1) [M+HCOO]-	CER	0.043288	↑
S-HEX-CER (d40:2) [M-H]-	CER	0.047847	↑
PI 40:5 [M-H]-	PI	0.043486	↑

p-values are reported after FDR correction. ↓: lipid species decreased from baseline; ↑: lipid species increased from baseline.

Despite individual differences, lipid reduction was graded between baseline, T4w and T12w (data not shown). Five polyunsaturated diacyl PC (PC 34:2, PC 36:2, PC 36:4, PC 37:6 and PC 38:4), two ether/vinyl ether forms (PC O-32:0 and (O-36:3) (P-36:2)) and one oxidized molecule (PC 34:1 (OH)) were reduced by the treatment. The analysis also revealed that these five reduced diacyl-PCs are a large proportion of total PC at baseline (range:38.6 to 49.2%; data not shown). Very interestingly, variance with its oxidized form PC 34:1 (OH), PC 34:1 (10.4 to 20.5% of total PC) was not significantly affected by PCSK9 inhibitor treatment. Seven SM, 5 CER and HEX-CER were significantly reduced at T12w. Contrary to what described for PC, SM and CER, reduction seems to be a general trend given that both medium- and long-chain saturated and unsaturated species were affected. The only exception was the two long-chain monounsaturated CER (d43:1 and d44:1) that were increased together with the S-HEX-CER (d40:2). Two PI species showed opposite trends as compared to baseline data: PI 38:5 was reduced while the PI 40:5 was increased. Consistent with the described TC reduction, CE 18:2 and CE 20:4, together accounting for 87.6% to 98.2% of total CE, were strongly reduced by the treatment. In contrast, neutral lipids DAG and TG were unaffected, indicating that the treatment with PCSK-9 inhibitor does not affect TG both quantitatively and qualitatively. Two exceptions are represented by odd-chain TG that were reduced. However, this is only a minute proportion of total TG (0.7 to 3.0%, data not shown). Although PE were not significantly affected, it displayed shorter and more saturated fatty acyl

chains compared to baseline (qualitative changes, **Table 3**). Likewise, compared to baseline, the unsaturation index of HEX-CER and lactosyl-(LAC)-CER was reduced.

Table 3: Average Chain Length (ACL) and Unsaturation Index (UI) for each lipid class at each time point.

Lipid class	ACL				UI			
	T ₀	T ₄	T ₁₂	(<i>p</i> -value)	T ₀	T ₄	T ₁₂	(<i>p</i> -value)
LPC	17,5178	17,4820	17,4140	0,644125	0,2203	0,2147	0,2000	0,683932
PC	35,6470	35,6681	35,6783	0,6839315	0,9930	1,0043	1,0048	0,81635
LPE	19,7342	19,7836	19,8026	0,881867	0,0197	0,0141	0,0127	0,906363
PE	37,4263	37,3464	37,2701	0,024802*	1,6802	1,5942	1,5630	0,002333*
PI	37,5724	37,5341	37,5332	0,698246	1,3583	1,3476	1,3451	0,771916
SM	37,9698	38,0673	38,0144	0,286808	1,4340	1,4550	1,4485	0,113967
CER	41,0776	41,0955	40,9025	0,4175	1,2107	1,2265	1,2168	0,609739
HEX-CER	38,8486	38,6879	38,8002	0,103829	1,2876	1,2578	1,2498	0,013582*
LAC-CER	34	34	34	1	1,0585	1,0696	1,0746	0,043693*
S-HEX-CER	35,3425	35,7382	35,4966	0,04639*	1,6535	1,6796	1,6500	0,527907
CE	18,8499	18,8671	18,8674	0,924687	2,7793	2,7927	2,7976	0,921739
DAG	36,3020	36,2523	36,1798	0,343138	2,6973	2,6425	2,5910	0,088299
TG	52,2924	52,2627	52,2426	0,938821	3,3240	3,2965	3,2587	0,795857

p-value after ANOVA. *: statistically significant.

3.4 Metabolomics Changes during Treatment with PCSK9 inhibitor

Major metabolic changes were detected in the plasma of the FH patients after the 12-week treatment with the PCSK9i. As many as 3300 molecular features were collected in the two different LC–MS modes (1700 in positive and 1600 in negative ionization modes). After visual validation of peak morphology and manual integration, and correction of the whole dataset, a total of 1221 compounds (607 and 614, respectively) emerged as having been affected by PCSK9i treatment. Of them, 97 molecular features showed significant treatment-related changes (ANOVA, $p < 0.05$). Based on the comparison of the m/z values and the corresponding MS/MS fragmentation spectra against different metabolomics databases, 26 compounds (**Table 4**) with a log fold-change (FC) ranging from -0.6 to 0.98 showed significant changes after 12 weeks (T12) of treatment (adj. p value < 0.05) (**Figure 7** and **Figure 8**).

Table 4. Metabolites identified by UHPLC-ESI-QTOF-MS that appeared significantly affected by 12-week treatment with PCSK9 inhibitor.

Mode	MW	m/z	Rt, min	Adjusted p-value	Log FC (T2/T0)	Putative Annotation
ESI+	428,364	429,372	12,91	0,000	-0,362	Cholesterol derivative
ESI+	173,985	174,993	0,84	0,029	0,276	Not identified
ESI+	183,087	184,095	0,69	0,029	0,641	Drug
ESI+	486,271	487,279	8,91	0,033	-0,174	PA (20:4/2:0)
ESI+	143,095	144,103	0,7	0,033	0,956	Proline betaine
ESI+	627,467	628,475	12,22	0,041	-0,598	Squalamine
ESI+	357,953	358,961	0,84	0,041	0,162	Not identified
ESI+	320,003	321,011	0,84	0,041	0,198	Not identified
ESI+	664,414	665,422	9,31	0,041	0,397	PA (22:6/12:0)
ESI+	133,996	135,004	0,84	0,041	0,196	Not identified
ESI+	301,962	302,97	0,84	0,041	0,323	Not identified
ESI+	523,363	524,371	8,91	0,041	-0,139	PAF C-16

ESI+	293,18	294,188	8,91	0,041	-0,114	Quifenadine
ESI+	165,077	166,085	0,7	0,041	0,978	L-Phenylalanine
ESI+	242,964	243,972	0,84	0,041	0,266	Not identified
ESI+	126,068	127,076	0,7	0,041	0,766	3-heptynoic acid
ESI+	543,33	544,338	7,64	0,041	-0,166	PC (20:4/0:0)
ESI+	131,07	132,077	0,66	0,041	0,214	Creatine
ESI+	523,365	524,373	8,73	0,042	-0,128	PC (0:0/18:0)
ESI+	363,971	364,979	0,84	0,045	0,147	Not identified
ESI+	281,157	282,165	8,91	0,045	-0,087	Xanomeline
ESI+	103,1	104,108	8,91	0,045	-0,113	Choline
ESI+	428,366	429,374	13,09	0,045	-0,204	(3beta,24R,24'R) - fucosterol epoxide
ESI+	187,064	188,072	2,65	0,045	0,128	Indoleacrylic acid
ESI+	117,059	118,067	2,65	0,045	0,127	Not identified
ESI-	351,214	350,206	6,3	0,023	0,233	Not identified

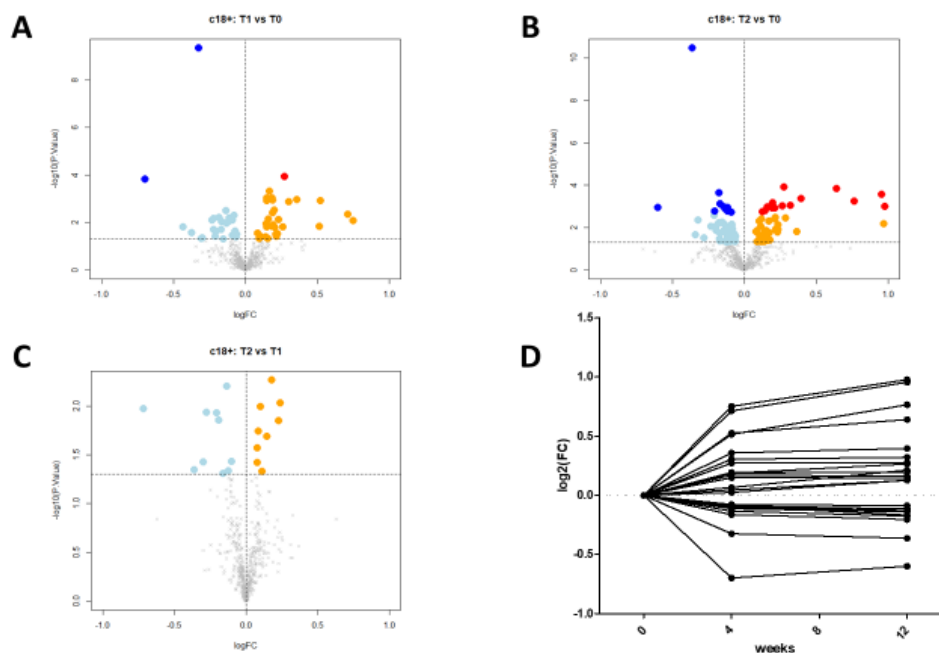


Figure 7. Volcano plots and scatter plot. The results of the statistical analysis for compounds analyzed in positive ion mode are summarized as a volcano plot of \log_2 fold-change (x-axis) versus $-\log_{10}$ p-values (y-axis), for three experimental designs: T1 vs. T0 (panel A), T2 vs. T0 (panel B), and T2 vs. T1 (panel C). Colored dots are the differentially abundant compounds: light blue and dark blue dots refer to compounds downregulated at p -value < 0.05 and adjusted p -value < 0.05 , respectively; orange and red dots are compounds upregulated at p -value < 0.05 and adjusted p -value < 0.05 , respectively. Scatter plot (panel D) shows the trend over time of the 19 differentially expressed compounds (adjusted p -value < 0.05).

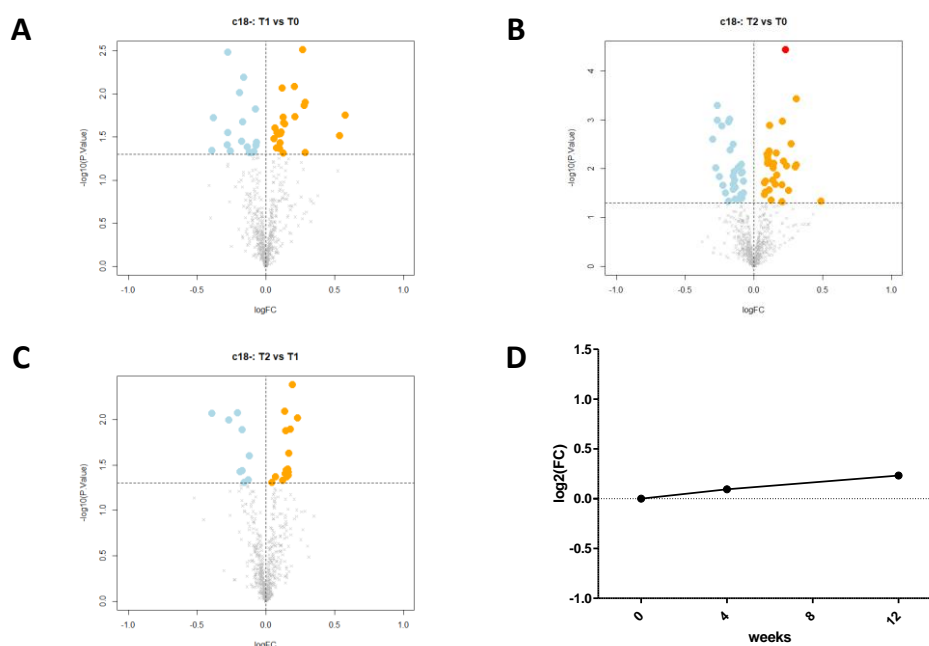


Figure 8. Volcano plots and scatter plot. The statistical analysis results for compounds analyzed in negative ion mode are summarized as a volcano plot of log₂ fold-change (x-axis) versus $-\log_{10}$ p-values (y-axis), for three experimental designs: T1 vs. T0 (panel A), T2 vs. T0 (panel B), and T2 vs. T1 (panel C). Colored dots are the differentially abundant compounds: light blue and dark blue dots are compounds downregulated at p-value < 0.05 and adjusted p-value < 0.05, respectively; orange and red dots are compounds upregulated at p-value < 0.05 and adjusted p-value < 0.05, respectively. Scatter plot (panel D) shows the trend over time of 19 differentially expressed compounds (adjusted p-value < 0.05). These data refer to the 5 compounds maximally modified after 12 weeks of treatment with Evolocumab[®], having a Benjamini–Hochberg false discovery rate-corrected p-value < 0.05.

With respect to such compounds, 9/26 were not identified. After adjusting for multiple comparisons, 5/26 metabolites were clearly identified: choline, platelet-activating factor 16 (PAF C16), creatine (Cr), indoleacrylic acid (IA), and indole. Of them (**Table 5**), both choline ($\log_2(\text{FC})$ T2/T0 = -0.113, adj. p-value = 0.045) and platelet-activating factor 16 (PAF C16) ($\log_2(\text{FC})$ T2/T0 = -0.139, adj. p-value = 0.041) were significantly reduced after a 12 week administration of the PCSK9i. In contrast, creatine (Cr) (\log_2 fold-change T2/T0 = 0.214, adj. p-value = 0.041), indoleacrylic acid (IA) (\log_2 fold-change T2/T0 = 0.128, adj. p-value = 0.045), and indole (\log_2 fold-change T2/T0 = 0.127, adj. p-value = 0.045) significantly increased following PCSK9i treatment. In keeping with this, lipidomic analysis following the administration of PCSK9i showed a significant reduction in PC; of 5 polyunsaturated diacyl PC (PC 34:2, PC 36:2, PC 36:4, PC 37:6, and PC 38:4); of two ether/vinyl ether forms of PC (PC O-32:0 and (O-36:3) (P-36:2), and of an oxidized PC molecule (PC 34:1 (OH), p values always <0.01).

Table 5. Identification of compounds that significantly increase (n = 3) and decrease (n = 2) after 12 weeks of treatment with PCSK9 inhibitor.

Mass	m/z	RT	Identified compound	Δppm	Log FC T2/T0
Increased from baseline					
131.07	132.0772	0.66	Creatine	3	LogFC = 0.214
187.064	188.0708	2.652	Indoleacrylic acid	1	LogFC = 0.128
117.059	118.0657	2.652	Indole	5	LogFC = 0.127
Reduced from baseline					
523.363	524.371	8.907	PAF C-16	0	LogFC = -0.139
103.0998	104.1071	8.907	Choline	0	LogFC = -0.113

3.5 Carotid stiffness and distensibility

During the 12-week treatment both systolic and diastolic blood pressure values remained stable, changing from 132±22 to 126±16 mmHg (p = 0.051) and from 76±8 to 77±9 mmHg (p = 0.550). At baseline assessment, the 25 subjects showed a carotid stiffness of 8.8 (IQR: 7.0-10.4) m/sec. After 12 weeks of treatment, carotid stiffness changed from 8.8 (IQR: 7.0-10.4) m/sec to 6.6 (IQR: 5.4-7.5) m/sec at T12_w corresponding to a median change of 21.4% (p < 0.001). In parallel, a significant increase in carotid distensibility was observed from 12.1 (IQR: 8.73-19.3) kPA⁻¹ × 10⁻³ at T₀ to 21.8 (IQR: 16.6-31.8) kPA⁻¹ × 10⁻³ at T12_w corresponding to a median change of 62.8% (p < 0.001). The prevalence of low carotid distensibility changed from 60% at baseline to 20% at T12_w (p = 0.011) (*Figure 9*).

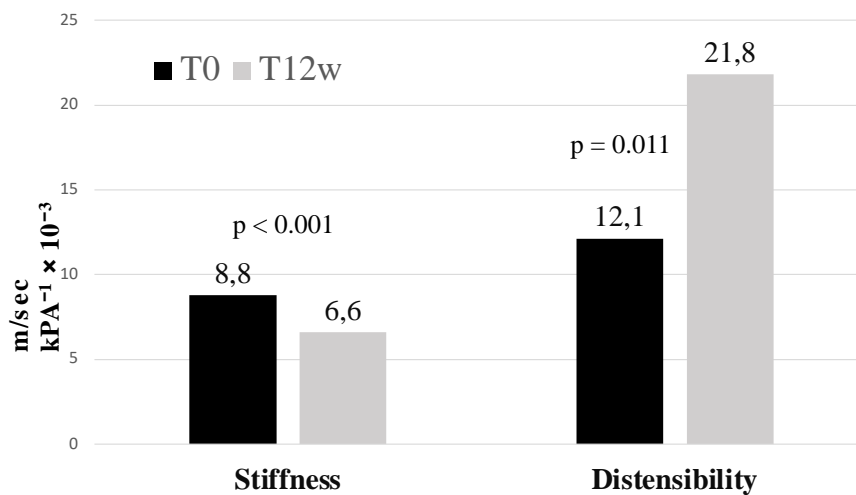


Figure 9: changes in carotid stiffness and distensibility from baseline to T12w

Changes in carotid stiffness and carotid distensibility showed an inverse significant correlation ($\rho = -0.998$, $p < 0.001$).

On-trial LDL-c levels showed a significant correlation with carotid stiffness ($\rho = 0.405$, $p = 0.004$) and carotid distensibility ($\rho = -0.407$, $p = 0.004$). Changes in carotid stiffness and carotid distensibility showed an inverse significant correlation ($\rho = -0.998$, $p < 0.001$).

Changes in LDL-c levels and in LDL score showed a significant correlation with carotid stiffness (Figure 10).

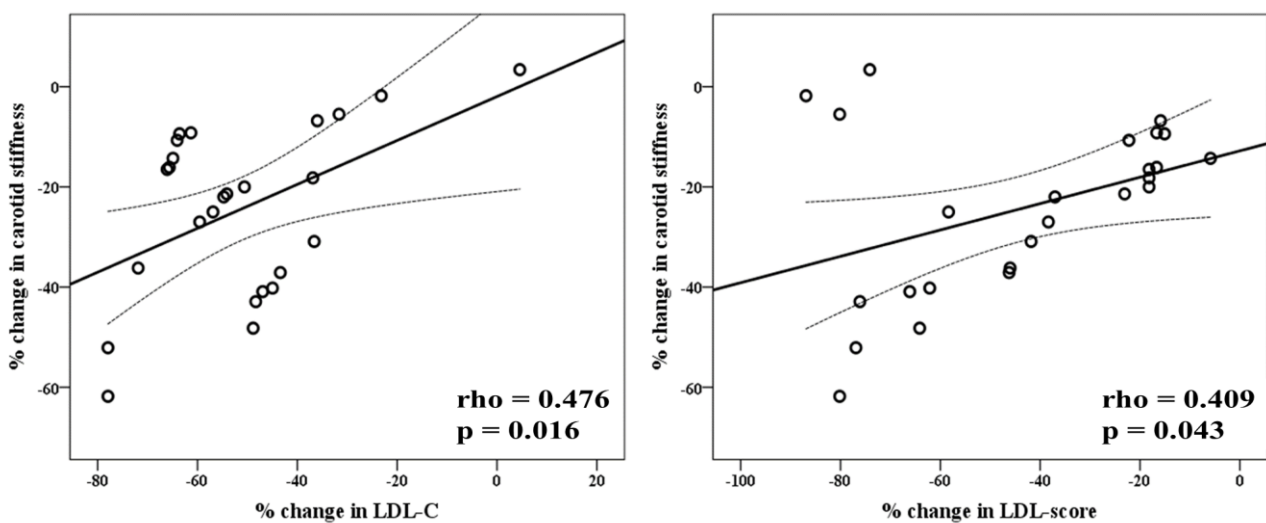


Figure 10: Scatter plot of correlation between percent change in low-density lipoprotein cholesterol (LDL-C) and LDL score with percent change in carotid stiffness during treatment with PCSK-9 inhibitor.

Given the potential influence of clinical and demographic characteristics and concomitant cardiovascular risk factor on changes in carotid stiffness and carotid distensibility, we performed sub-group analyses entirely confirming results obtained in the primary analysis (*Figure 11*).

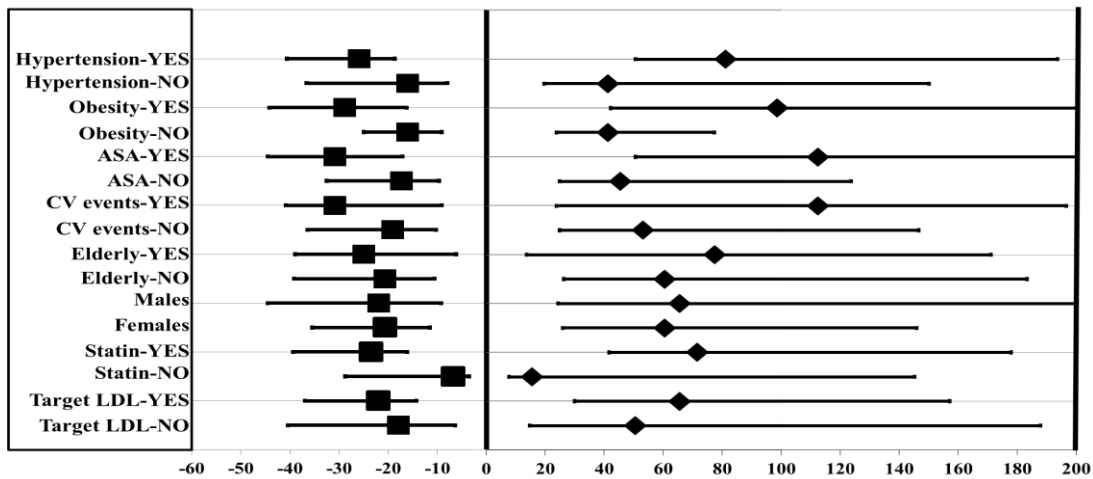


Figure 11: Median percent changes in carotid stiffness and carotid distensibility from baseline values to 12 weeks of therapy with PCSK9 inhibitors in the study population stratified according to predefined study sub-groups

A more pronounced reduction of carotid stiffness and increase in carotid distensibility was observed in patients with heterozygote mutation of *LDLR* as compared to compound heterozygotes/double heterozygotes subjects (*Figure 12*).

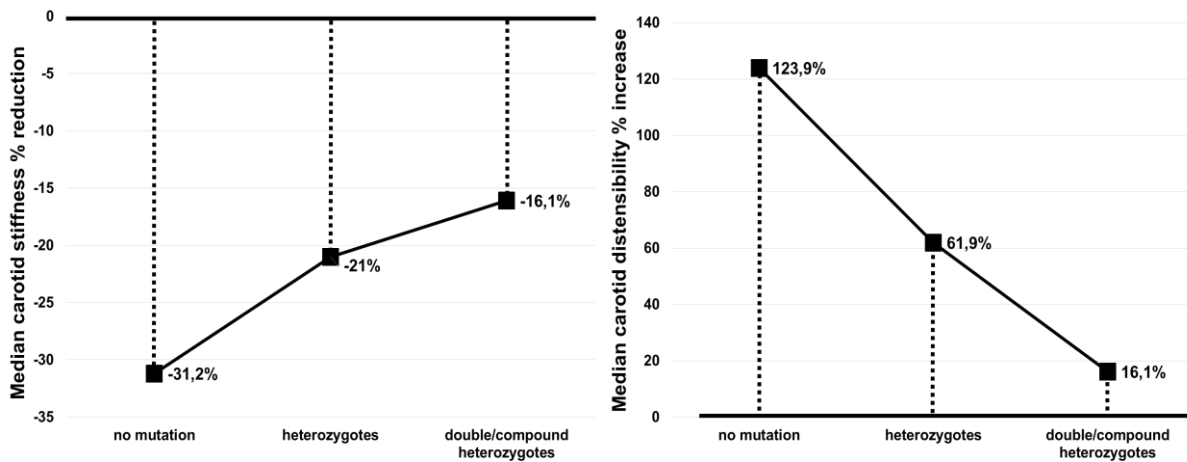


Figure 12: Changes in carotid stiffness (label A) and carotid distensibility (label B) during treatment with PCSK9 inhibitor stratifying patients according to genotype.

In a multivariate analysis including age, gender, BMI cardiovascular events, we found that on trial LDL-c, hypertension, diabetes were independently associated with carotid stiffness and carotid distensibility (*Table 6*). Moreover, changes in LDL score were independently associated with changes in carotid stiffness from baseline values to T12_w ($\beta = 0.429$, $p = 0.041$).

Table 6: Linear regression analysis. Association of clinical and laboratory parameters with carotid stiffness and distensibility.

	Carotid Stiffness	Carotid Distensibility
LDL-C	$\beta = 0.511$ $p < 0.001$	$\beta = - 0.506$ $p = 0.001$
Diabetes	$\beta = 0.346$ $p = 0.007$	$\beta = - 0.294$ $p = 0.040$
Hypertension	$\beta = 0.391$ $p = 0.004$	$\beta = - 0.366$ $p = 0.018$

At T104w, carotid stiffness evaluation was performed in 16 patients, because 6 patients were lost at follow-up, 1 patient had a new-onset arterial hypertension, 1 patient changed the lipid lowering treatment adding evinacumab and 1 patient dead because of laryngeal cancer. This long-term

assessment showed a consistent and progressive improvement of carotid stiffness and carotid distensibility as compared to baseline values (*Figure 12*).

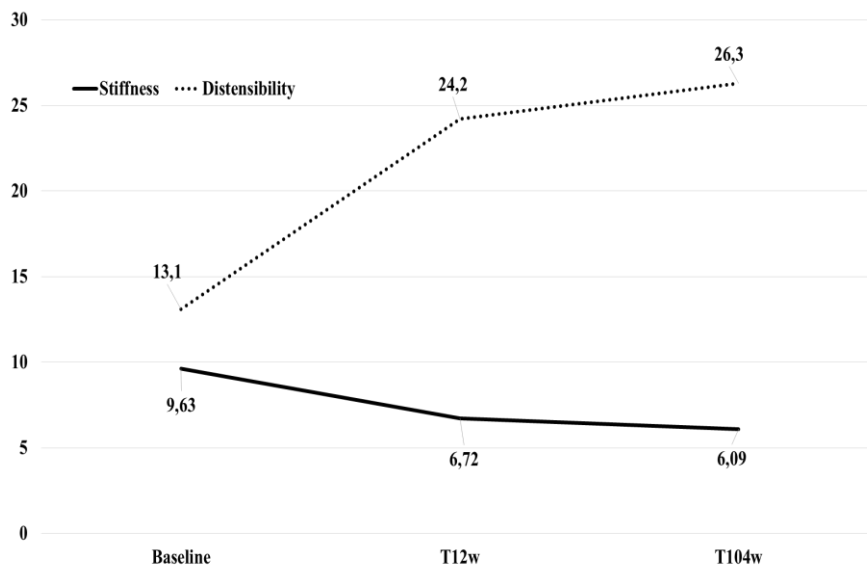


Figure 12: Changes in carotid stiffness and carotid distensibility from baseline values to week 12 and week 104 during treatment with PCSK9 inhibitor.

3.6 Oxidative stress markers

When assessing changes in oxidation markers, we documented a progressive decrease in 11-TXB2 (18%) and 8-iso-PGF2 α (17%) from baseline values (Fig. 2) to T12w, with a significant correlation with changes in LDL score (11-TXB2: $\rho = 0.506$, $p = 0.016$ and 8-iso-PGF2 α : $\rho = 0.511$, $p = 0.018$). After adjusting for age, gender, BMI, cardiovascular events, hypertension, and diabetes change in LDL score was an independent predictor of changes in 8-iso-PGF2 α from baseline values to T12w ($\beta = 0.778$, $p = 0.012$), but not of changes in 11 TXB2.

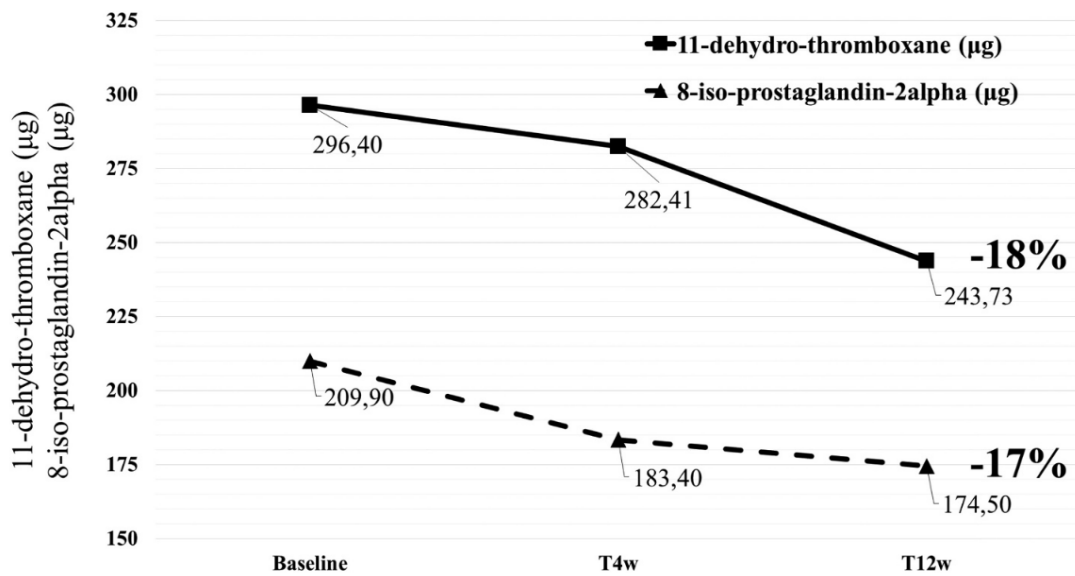


Figure 13: Changes in 11-dehydro-thromboxane (µg), 8-isoprostaglandin-2alpha (µg) and 2,3-dinor-8-isoprostaglandin-2alpha (µg) during treatment with PCSK-9 inhibitor. Note to Fig.13 all values have been adjusted for creatinine level.

3.7 Endothelial function

At baseline assessment, the 25 subjects showed a BAD of 4.16 ± 0.95 mm. FMD was $4.78\% \pm 2.27$, with an AUC 4418 (IQR: 2240.9–8045.1) and RHI 2.37 ± 1.23 . After 4 weeks of treatment with PCSK-9i (T4w) no significant changes in BAD occurred (from 4.16 ± 0.95 mm to 4.16 ± 0.78 mm, $p = 0.985$). FMD changed from $4.78\% \pm 2.27$ to $9.43\% \pm 4.29$ ($p < 0.001$) and AUC increased from 4418 (IQR: 2240.9–8045.1) to 10,228 (IQR: 5780.9–13,536.9, $p = 0.002$), whereas no significant changes were observed in RHI (from 2.37 ± 1.23 to 3.21 ± 1.71 , $p = 0.061$). After 12 weeks of treatment with PCSK-9i (T12w) BAD was similar to baseline values (4.16 ± 0.95 mm vs 4.17 ± 0.86 mm, $p = 0.924$). FMD changed from $4.78\% \pm 2.27$ to $10.6\% \pm 5.89$ ($p < 0.001$), RHI from 2.37 ± 1.23 to 3.76 ± 1.36 ($p < 0.001$) with AUC increasing from 4418 (IQR: 2240.9–8045.1) to 14,248.1 (IQR: 8684.1–21,053.8) ($p < 0.001$) (Figure 14). The prevalence of low-RHI changed from 36.0% at baseline to 16.0% at T4w (p vs baseline 0.116) and to 8% at T12w (p vs baseline 0.027).

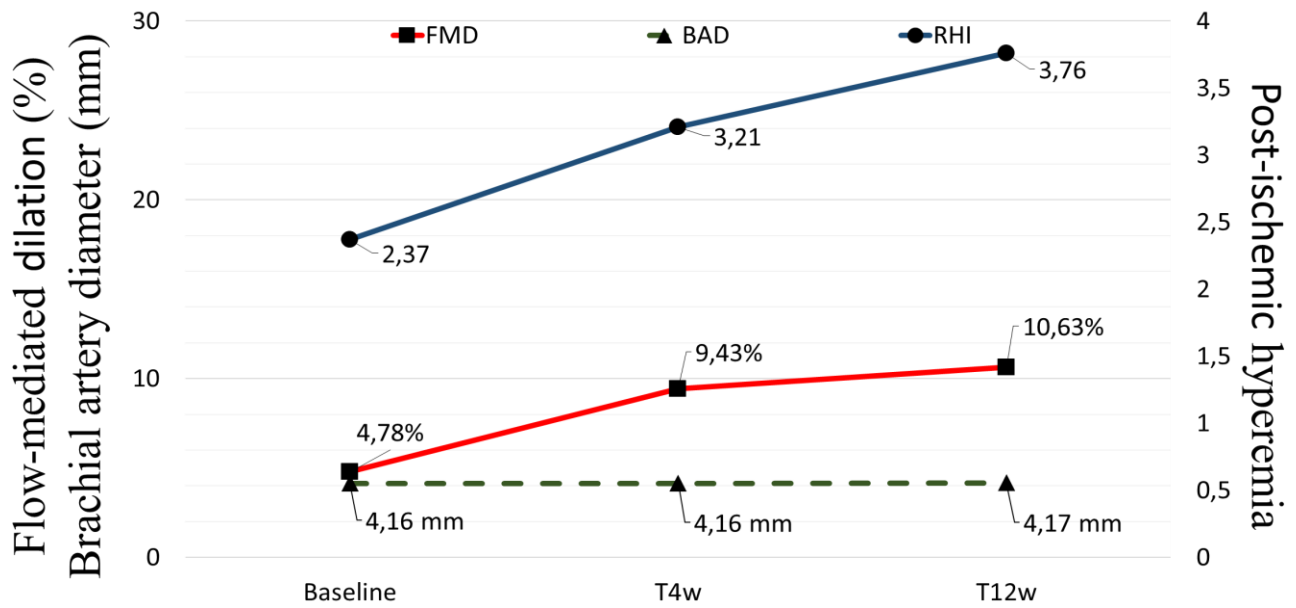


Figure 14: Changes in brachial artery diameter (BAD), flow-mediated dilation (FMD) and Reactive Hyperemia Index (RHI) expressed by shear rate area under the curve during treatment with PCSK-9 inhibitor. Note to Fig. 3: T4w: 4 weeks after starting treatment with PCSK-9 inhibitor; T12w: 12 weeks after starting treatment with PCSK-9 inhibitor; *: statistically significant change as compared to baseline values.

To explore the potential influence of demographic and clinical characteristics and concomitant cardiovascular risk factor on changes in FMD and RHI, we performed sub-group analyses entirely confirming results obtained in the primary analysis (Figure 15).

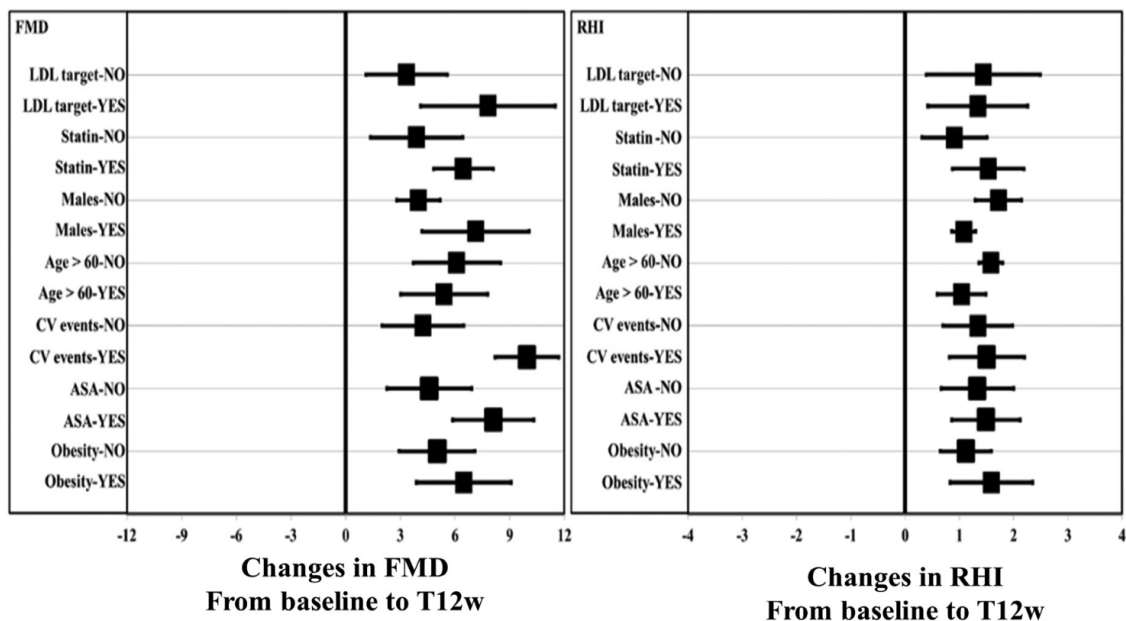


Figure 15 Changes in flow-mediated dilation and reactive hyperemia index from baseline values to 12 weeks of therapy with PCSK-9 inhibitors in the study population stratified according to predefined sub-groups.

FMD: flow-mediated dilation; RHI: reactive hyperemia index; LDL: low-density lipoprotein; CV: cardiovascular; ASA: aspirin

FMD values showed an inverse and significant correlation with LDL-C levels assessed at different time-points ($\rho = -0.391$, $p = 0.001$).

Changes in 11-TXB2 and 8-iso-PGF2 α from baseline values significantly correlated with changes in FMD (11-TXB2: $\rho = -0.436$, $p = 0.033$ and 8-iso- PGF2 α : $\rho = -0.511$, $p = 0.018$), but after adjusting for age, gender, BMI, cardiovascular events, hypertension and diabetes, changes in LDL score was the only independent predictor of changes in FMD from baseline values to T12w ($\beta = -0.846$, $p = 0.015$).

4. Discussion

In the present study, we documented that in a FH patients cohort therapy with PCSK9i on top of standard lipid lowering therapy led to significant reduction of LDL-C. After a 12-week treatment, patients reported a 49% LDL-C reduction, with LDL-C target being achieved by 74% of subjects receiving PCSK9i + statin \pm ezetimibe and by 17% of those treated with PCSK9i \pm ezetimibe. These results consistently confirm the widely documented LDL-C reduction rate reported during treatment with PCSK9i.^{48, 49} Beyond LDL-C reduction we documented also changes in LDL diameter and composition expressed as reduction in LDL score, a parameter correlated with LDL diameter and, in turn, with sd-LDL levels. LDL-C changes were accompanied by a significant improvement in endothelial function and reduction of carotid stiffness. Furthermore, we showed that sd-LDL reduction is associated to changes in oxidation markers and subclinical atherosclerosis improvement. However, we found an extremely limited modification in LDL score in compound heterozygote/double heterozygote patients as compared to those heterozygotes for single mutation of *LDLR*. This is plausible by a pathophysiological point of view, considering the mechanism of action of PCSK9 inhibitors, that induce an up regulation in LDL receptor, following the inhibition of PCSK9-mediated degradation. In patients with heterozygote/double heterozygote *LDLR*

mutation, receptor function could be seriously comprised, so up-regulation of LDL receptor expression could be ineffective.

The significant reduction in sd-LDL, known to be more susceptible to oxidative modification, to have a higher affinity for the arterial wall and widely recognized as predictors of CV events,^{67, 75, 76} potentially could be related to endothelial function improvement and arterial wall modifications leading to arterial stiffness regression and arterial wall distensibility augmentation. Extending and confirming this finding, we observed a significant correlation between changes in LDL score and changes in 8-iso-PGF₂α, a recognized marker of lipid peroxidation, endothelial activation and platelet reactivity.⁷⁷ As an ancillary finding, we also documented a slight but significant reduction in Lp(a) from 69.3 mg/dl at baseline to 41.7 mg/dl at T12w. Lp(a) is known to have a highly atherogenic effect and to be an independent predictor of CV events.⁷⁸ In detail, each 1 standard deviation increase in Lp(a) levels can raise the hazard ratio for cardiovascular events by 1.1–1.2.⁷⁹ In the present study, although median changes in Lp(a) were <10%, 32% of subjects reported a Lp(a) reduction > 25% compared with baseline values. On this hand, it is noteworthy to highlight that Lp(a), by inhibiting the feedback mechanism that accelerates plasmin formation on vascular cells, might be involved both in atherogenesis process and in thrombotic risk⁸⁰. This is somehow supported by a recent post hoc analysis of FOURIER and ODYSSEY OUTCOMES trial.⁸¹

Besides the lipid-lowering effect of PCSK9i, in the present study we documented a significant improvement in subclinical atherosclerosis markers (endothelial function and arterial stiffness), established predictors of CV and cerebrovascular morbidity and mortality,¹⁸ particularly in FH patients.⁸²

The exact mechanism by which PCSK9 inhibitor exerts a beneficial effect in improving endothelial function and carotid stiffness is still not completely described. Surely, lowering LDL-C levels represents one mechanism by which a subclinical atherosclerosis reduction can be achieved. Several literature data suggested that lipid-lowering therapies, by reducing oxidative stress and balancing

nitric oxide synthase (eNOS)/nitric oxide synthase (iNOS) ratio, lead to an improvement of endothelial function.^{83,84} Thus, it can be expected that lipid-lowering therapies may induce functional and structural modifications in artery wall and endothelial function, positively influencing subclinical atherosclerosis. In line with this hypothesis, we observed a correlation between LDL levels and carotid stiffness and, such an association was confirmed after adjusting for potential confounders.

These changes were also accompanied by reduction in several atherogenic lipid species and in changes in metabolites related to platelets activation proving for the first time the potential molecular and metabolic basis relative to pleiotropic effects of PCSK9i.

The untargeted lipidomic analysis showed a significant reduction of SM, PC, CE, LAC-CER, HEX-CER, and of some PI after 12 weeks treatment with evolocumab 140 mg. At the best of our knowledge, only two studies (one in humans⁸⁵ the other one in humans and mice⁸⁶) reported the effects of treatment with PCSK9i at level of individual lipid species. Our results are in line with a recent study by Hilvo et al. showing a significant reduction in the class of sphingolipids and cholesterol esters due to PCSK9 inhibition.⁸⁵ Among such lipid classes, SM, CER and CE were maximally affected by the treatment. Supporting the results of the present study, a clear reduction of SM, LAC-CER and CE in plasma has been demonstrated in KO mice for PCSK9 and in human carriers of the LOF mutation of PCSK9.⁸⁷

Raised levels of SM and CER are independently associated with cardiovascular risk.⁸⁷⁻⁸⁹ LAC-CER is thought to play a role both in intimal medium proliferation and in coronary endothelial dysfunction through the reduction of NO production.⁹⁰ Moreover, plasma CER levels predict CV death in patients with stable CAD and acute coronary syndromes beyond LDL-cholesterol.⁸⁸ Studies in mice show that SM are involved in the early phases of atherosclerosis through mechanisms involving signal transduction pathways that affect the proliferation of ECs and the formation of foam cells⁸⁹ Studies on KO mice for LDL-R in which the bone marrow of KO mice for the enzyme

sphingomyelin synthase 1 (SMS) was transplanted, showed a reduction in atherosclerosis at the level of the aorta. The absence of the SMS enzyme in the monocyte macrophage system reduces atherosclerosis progression, arguing for a role of SM in atherosclerosis independent of the LDLR.⁹¹

In keeping with this, activation of sphingomyelinase by the activated endothelium and by plaque macrophages is implicated in the retention and aggregation of APOB-lipoproteins and hence in facilitating adherence of APOB-lipoproteins to the arterial matrix, a key mechanism in atherogenesis.⁹² Moreover, CER plays a central role in sphingolipid metabolism. Once synthesized, CER triggers the activity of sphingomyelinase, thus releasing oleic acid by cytosolic phospholipase A 2 (cPLA 2), and in turn increasing CE production.⁹³ The activation of cPLA 2 in platelets is implicated in the release of arachidonic acid, indicating its potential role in platelet aggregation.^{94, 95}

Together, the pathophysiological mechanism through which PCSK9 inhibition, and the consequent up-regulation of LDL-R, modifies the lipidome seems to be related to an indirect mechanism.

Oxidized LDL (oxLDL) acts as a stimulus for the de novo synthesis of SM and CER through the activation of the key enzyme SMS.⁸⁹ Experimental evidence shows that the de novo synthesis of CER is involved in cholesterol esterification.⁸⁹ Together with oxidative modifications in LDL particles, cholesterol esterification exerts antigenic effects and, by activating both innate and adaptive immunity,⁹⁶ promotes atherosclerosis-associated inflammation. The present data suggest that oxLDL stimulate the de novo synthesis of CER, which promotes the hydrolytic activity of cPLA 2 to release oleic acid, thus increasing cholesterol esters production.⁸⁹

By employing untargeted metabolomics analysis, we have found significant reductions in the plasma levels of PAF C16, of PC, and of choline following 12-week administration of PCSK9i. PC is the most abundant phospholipid species in mammals, accounting for about 50% of total phospholipids. It is usually found in the outer membrane leaflet and exhibits bilayer-forming properties. PE is the second most abundant phospholipid in mammalian membranes, accounting for 20-30% of total phospholipids.⁹⁷ It is usually found in the inner membrane leaflet and is a non-

bilayer forming lipid. The PC/PE ratio is important for a correct membrane integrity and function.⁹⁸ PC is synthesized in the liver and approximately 70% of PC derives from the cytidine-diphosphate-choline: 1,2-diacylglycerol choline phosphotransferase (CDP-choline) enzyme (the *Kennedy pathway*), the remaining 30% being synthesized via phosphatidylethanolamine N-methyltransferase (*PEMT*) pathway.⁹⁹ At variance with the PEMT pathway where PC derives from three sequential methylations of ethanolamine and PE consumption,^{100, 101} PC biosynthesis via the Kennedy pathway requires choline.¹⁰²⁻¹⁰⁵ This metabolite was significantly reduced after 12-week administration of PCSK9i. Neither choline nor PC reductions were associated with significant variations in terms of PE, in this setting. Thus, rather for the PEMT pathway, the combined data argue for the Kennedy pathway as being affected after the administration of PCSK9i. The cellular depletion of PC influences the synthesis and HDL transport by the liver.¹⁰⁶ On the other hand, while further data are needed to elucidate the underlying mechanism(s) of its significant reduction in this setting, it is important to emphasize that choline is involved in lipoprotein metabolism.¹⁰⁷ Choline metabolism is important in the regulation of plasma cholesterol levels.¹⁰⁸ It is remarkable that choline deficiency is associated with atheromatous changes in aorta, carotid and coronary arteries,¹⁰⁹ and choline exclusion from the diet inhibits the assembly and secretion of very low-density lipoproteins (VLDL) from hepatocytes.^{110, 111}

Like choline and PC, PAF was reduced in plasma from FH patients after 12-week administration of PCSK9i. The multifaceted spectrum of biological and pharmacological effects of PAF, including the ability to influence the function of platelets confers additional pathophysiological relevance to the present results.¹¹² Through the remodelling pathway, PC is converted by phospholipase A2 to PAF and lyso-derivatives, both exerting platelet activating capacities (**Figure 16**).¹¹³

C16 PAF (Platelet activating factor, 1-O-Hexadecyl-2-acetyl-sn-glycero-3-phosphocholine 1-O-alkyl-2-acetyl-sn-glycero-3-phosphocholine) is a potent mediator of neutrophil migration, and the production of reactive oxygen species, and interleukin-6 in human macrophages.

In addition to being involved in these well-known events in the initiation and progression of atherosclerosis, PAF plays a key role in platelet function by directly triggering aggregation and potentiating the effects of sub-threshold concentrations of other agonists.^{114, 115}

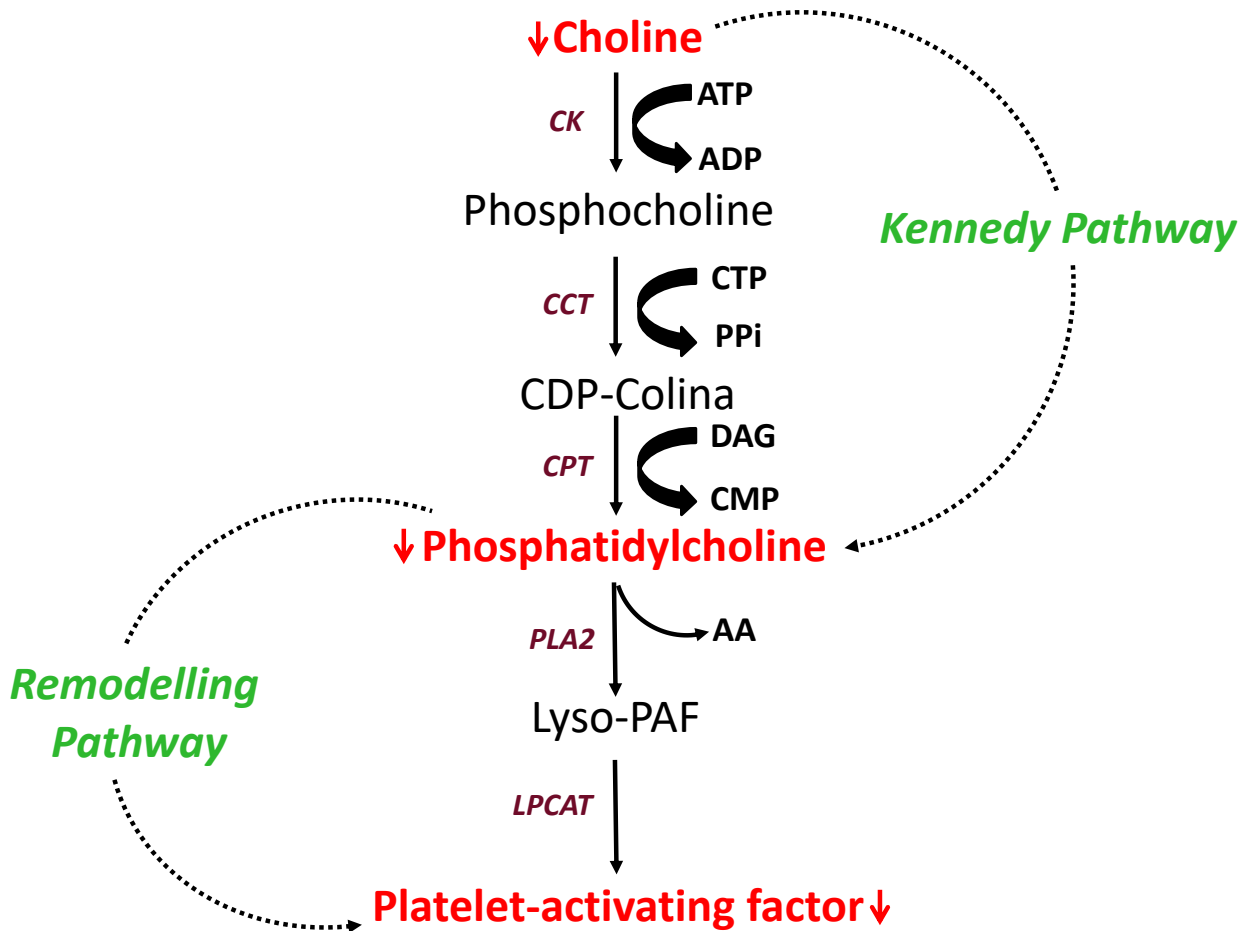


Figure 16. Regulation of Kennedy and Remodelling pathways: PCSK9 inhibitor treatment blocks platelet activating factor biosynthesis by regulating the Kennedy and remodelling pathways. Choline reduction reduces phosphatidylcholine (PC) synthesis resulting in reduced platelet activating factor (PAF) production.

Abbreviations: CK= choline kinase; CTP=cytidine triphosphate; CCT= CTP:phosphocholine cytidyltransferase; CDP-choline=cytidine diphosphocholine; CPT=CDP-choline:1,2-diacylglycerol choline-phosphotransferase DAG= diacylglycerol PLA2= phospholipase a 2 AA= arachidonic acid LPCAT= Lysophosphatidylcholine acyltransferase

The actions of this agent on the cardiovascular system are mediated by a specific receptor belonging to the seven transmembrane-spanning G-protein-linked receptors family.¹¹² In the present study we documented a significant reduction in PAF C16 in the plasma samples from these patients in parallel with reduction of 11-TXB2 and 8-iso-PGF2 α levels. The relevance of this finding is further supported by the known direct relationship between in vivo platelet activation and circulating

plasma levels of PCSK9.¹¹⁶ Further dedicated studies are needed to explore vivo effects on platelets reactivity in hypercholesterolemic subjects treated by PCSK9 inhibitors and a dedicated trial is ongoing.¹¹⁷ Our study might represent a start point to design targeted multi-omics on bigger population to fully explore and confirm potential pleiotropic effects of PCSK9 inhibition.

Some potential limitations of the present study need to be discussed. Most of patients included in the present study have concomitant CV risk factors, potentially impacting on evaluation of subclinical atherosclerosis markers. To overcome this potential source of heterogeneity, sub-group analyses were performed and showed that patients not receiving statins represented the only clinical subset reporting a less significant reduction in markers of subclinical atherosclerosis, thus suggesting a cooperation between statins and PCSK9 inhibitors. This hypothesis is also supported by previous studies showing that PCSK9 inhibitors reduced LDL-C levels of about 50% when used alone and about 70% when used together with statins.²⁸ A hypothetical mechanism of a synergic effect of association between statins and PCSK9i is due to increased plasma levels of PCSK9 in patients treated with statins alone. This effect is secondary to the activation of sterol responsive element binding protein (SREBP) pathway because of the inhibition of cholesterol biosynthesis. Thus, patients receiving chronic statin therapy have higher levels of PCSK9 and then a more marked response to PCSK9i.¹¹⁸ On the other hand, the significant improvement in subclinical atherosclerosis markers consistently found in all the other sub-groups considered, suggests that PCSK9i treatment leads to a reduction of the CV risk regardless of the presence of concomitant CV risk factors.

In our sample, we documented a trend toward a reduction in SBP during treatment with PCSK9i. We excluded any modification in antihypertensive treatment during study period to exclude a potential impact on results. This issue needs to be specifically addressed in future studies.

The lack of a control group might represent a limitation of the present study. However, PCSK9i can be used only in patients not achieving target LDL-C levels under maximal tolerated lipid lowering

treatment. Thus, a potential control group should be represented by not eligible to treatment with PCSK9i or refusing this treatment. These hypothetical controls are not likely to be comparable to cases. Overall, the pre-post observational design allows for partly overcome the intrinsic inter-individual heterogeneity, with each patient being the control of himself. Furthermore, another potential limitation of subgroup analysis of the study is represented by the small number of patients in each subcategory.

6. Conclusions:

In conclusion, this study showed, for the first time an effect of 12 weeks of treatment with PCSK9i on subclinical atherosclerosis markers. Moreover, we found that sd-LDL reduction is related to changes in subclinical atherosclerosis, thus suggesting a potential impact for changes in lipoprotein composition as a mechanism for CV risk reduction. We further documented that, LDL reduction appears to be an important factor in the modification of plasma phospholipids. On this hand the improved LDL catabolism and the related reduction in APO-B containing lipoproteins is likely to be involved in lipidomic changes in patients treated with PCSK9i. These data rule out direct mechanisms of PCSK9 inhibition on lipidomic modifications and argue for a multifaceted system leading to vascular improvement in subjects treated with a PCSK9i, in line with clinical data showing subclinical atherosclerosis regression documented in patients receiving a PCSK9i.

Additionally, taking advantage of untargeted metabolomics, we first provide evidence of a concomitant reduction of both inflammation and platelet activation factors in FH patients. These pleiotropic effects could explain, at least in part, the CV risk reduction and atherosclerotic plaque regression observed following a treatment with PCSK9i. The data here reported also support the concept that untargeted multi-omics analysis is major direction to be pursued to widely investigate treatment effects and explore new clinical application of such treatment. Obviously, all biochemical and biological conclusions based on our small sample size, need to be confirmed in a larger number of participants with targeted analysis. Our study might represent a start point to design targeted

multi-omics on bigger population to fully explore and confirm potential pleiotropic effects of PCSK9 inhibition.

7. Acknowledgements:

I would like to thank all the professors and researchers who participated directly in realizing this study project:

- Prof. Matteo Di Minno;
- Prof. Paolo Rubba
- Prof. Elena Tremoli;
- Prof. Viviana Cavalca;
- Prof. Gualtiero Colombo;
- Dr. Alessandro Di Minno;
- Dr. Marco Gentile;
- Dr. Andrea Anesi;
- Dr. Benedetta Porro;
- Dr. Roberta Clara Orsini;
- Dr. Maria Tripaldella;
- Dr. Susanna Fiorelli;
- Dr. Sonia Elinigini.

"If I have seen further (than others), it is by standing on the shoulders of giants." (Isaac Newton 1675)

References

1. Singh S and Bittner V. Familial hypercholesterolemia--epidemiology, diagnosis, and screening. *Current atherosclerosis reports*. 2015;17:482.
2. Cuchel M, Bruckert E, Ginsberg HN, Raal FJ, Santos RD, Hegele RA, Kuivenhoven JA, Nordestgaard BG, Descamps OS, Steinhagen-Thiessen E, Tybjaerg-Hansen A, Watts GF, Averna M, Boileau C, Boren J, Catapano AL, Defesche JC, Hovingh GK, Humphries SE, Kovanen PT, Masana L, Pajukanta P, Parhofer KG, Ray KK, Stalenhoef AF, Stroes E, Taskinen MR, Wiegman A, Wiklund O, Chapman MJ and European Atherosclerosis Society Consensus Panel on Familial H. Homozygous familial hypercholesterolaemia: new insights and guidance for clinicians to improve detection and clinical management. A position paper from the Consensus Panel on Familial Hypercholesterolaemia of the European Atherosclerosis Society. *European heart journal*. 2014;35:2146-57.
3. Akioyamen LE, Genest J, Shan SD, Reel RL, Albaum JM, Chu A and Tu JV. Estimating the prevalence of heterozygous familial hypercholesterolaemia: a systematic review and meta-analysis. *BMJ Open*. 2017;7:e016461.
4. Mach F, Baigent C, Catapano AL, Koskinas KC, Casula M, Badimon L, Chapman MJ, De Backer GG, Delgado V, Ference BA, Graham IM, Halliday A, Landmesser U, Mihaylova B, Pedersen TR, Riccardi G, Richter DJ, Sabatine MS, Taskinen MR, Tokgozoglu L, Wiklund O and Group ESCSD. 2019 ESC/EAS Guidelines for the management of dyslipidaemias: lipid modification to reduce cardiovascular risk. *European heart journal*. 2020;41:111-188.
5. Rubba P, Gentile M, Marotta G, Iannuzzi A, Sodano M, De Simone B, Jossa F, Iannuzzo G, Giacobbe C, Di Taranto MD and Fortunato G. Causative mutations and premature cardiovascular disease in patients with heterozygous familial hypercholesterolaemia. *European journal of preventive cardiology*. 2017;24:1051-1059.
6. Goldstein JL and Brown MS. The LDL receptor locus and the genetics of familial hypercholesterolemia. *Annu Rev Genet*. 1979;13:259-89.
7. Di Taranto MD, Giacobbe C and Fortunato G. Familial hypercholesterolemia: A complex genetic disease with variable phenotypes. *Eur J Med Genet*. 2020;63:103831.
8. Soutar AK and Naoumova RP. Mechanisms of disease: genetic causes of familial hypercholesterolemia. *Nat Clin Pract Cardiovasc Med*. 2007;4:214-25.
9. Varret M, Abifadel M, Rabes JP and Boileau C. Genetic heterogeneity of autosomal dominant hypercholesterolemia. *Clin Genet*. 2008;73:1-13.

10. Abifadel M, Varret M, Rabes JP, Allard D, Ouguerram K, Devillers M, Cruaud C, Benjannet S, Wickham L, Erlich D, Derre A, Villegier L, Farnier M, Beucler I, Bruckert E, Chambaz J, Chanu B, Lecerf JM, Luc G, Moulin P, Weissenbach J, Prat A, Krempf M, Junien C, Seidah NG and Boileau C. Mutations in PCSK9 cause autosomal dominant hypercholesterolemia. *Nat Genet.* 2003;34:154-6.
11. Cohen JC, Boerwinkle E, Mosley TH, Jr. and Hobbs HH. Sequence variations in PCSK9, low LDL, and protection against coronary heart disease. *The New England journal of medicine.* 2006;354:1264-72.
12. Barale C, Melchionda E, Morotti A and Russo I. PCSK9 Biology and Its Role in Atherothrombosis. *Int J Mol Sci.* 2021;22.
13. Fouchier SW, Dallinga-Thie GM, Meijers JC, Zelcer N, Kastelein JJ, Defesche JC and Hovingh GK. Mutations in STAP1 are associated with autosomal dominant hypercholesterolemia. *Circ Res.* 2014;115:552-5.
14. Soutar AK, Naoumova RP and Traub LM. Genetics, clinical phenotype, and molecular cell biology of autosomal recessive hypercholesterolemia. *Arteriosclerosis, thrombosis, and vascular biology.* 2003;23:1963-70.
15. Talmud PJ, Shah S, Whittall R, Futema M, Howard P, Cooper JA, Harrison SC, Li K, Drenos F, Karpe F, Neil HA, Descamps OS, Langenberg C, Lench N, Kivimaki M, Whittaker J, Hingorani AD, Kumari M and Humphries SE. Use of low-density lipoprotein cholesterol gene score to distinguish patients with polygenic and monogenic familial hypercholesterolaemia: a case-control study. *Lancet.* 2013;381:1293-301.
16. Risk of fatal coronary heart disease in familial hypercholesterolaemia. Scientific Steering Committee on behalf of the Simon Broome Register Group. *BMJ.* 1991;303:893-6.
17. Khera AV, Won HH, Peloso GM, Lawson KS, Bartz TM, Deng X, van Leeuwen EM, Natarajan P, Emdin CA, Bick AG, Morrison AC, Brody JA, Gupta N, Nomura A, Kessler T, Duga S, Bis JC, van Duijn CM, Cupples LA, Psaty B, Rader DJ, Danesh J, Schunkert H, McPherson R, Farrall M, Watkins H, Lander E, Wilson JG, Correa A, Boerwinkle E, Merlini PA, Ardissino D, Saleheen D, Gabriel S and Kathiresan S. Diagnostic Yield and Clinical Utility of Sequencing Familial Hypercholesterolemia Genes in Patients With Severe Hypercholesterolemia. *Journal of the American College of Cardiology.* 2016;67:2578-89.
18. Daiber A, Steven S, Weber A, Shuvaev VV, Muzykantov VR, Laher I, Li H, Lamas S and Munzel T. Targeting vascular (endothelial) dysfunction. *Br J Pharmacol.* 2017;174:1591-1619.

19. Aggoun Y, Bonnet D, Sidi D, Girardet JP, Brucker E, Polak M, Safar ME and Levy BI. Arterial mechanical changes in children with familial hypercholesterolemia. *Arteriosclerosis, thrombosis, and vascular biology*. 2000;20:2070-5.
20. d'Alessandro E, Becker C, Bergmeier W, Bode C, Bourne JH, Brown H, Buller HR, Ten Cate-Hoek AJ, Ten Cate V, van Cauteren YJM, Cheung YFH, Cleuren A, Coenen D, Crijns H, de Simone I, Dolleman SC, Klein CE, Fernandez DI, Granneman L, van THA, Henke P, Henskens YMC, Huang J, Jennings LK, Jooss N, Karel M, van den Kerkhof D, Klok FA, Kremers B, Lammle B, Leader A, Lundstrom A, Mackman N, Mannucci PM, Maqsood Z, van der Meijden PEJ, van Moorsel M, Moran LA, Morser J, van Mourik M, Navarro S, Neagoe RAI, Olie RH, van Paridon P, Posma J, Provenzale I, Reitsma PH, Scaf B, Schurgers L, Seelig J, Siegbahn A, Siegerink B, Soehnlein O, Soriano EM, Sowa MA, Spronk HMH, Storey RF, Tantiwong C, Veninga A, Wang X, Watson SP, Weitz J, Zeerleder SS, Ten Cate H and Scientific Reviewer C. Thrombo-Inflammation in Cardiovascular Disease: An Expert Consensus Document from the Third Maastricht Consensus Conference on Thrombosis. *Thromb Haemost*. 2020;120:538-564.
21. Giannotta M, Trani M and Dejana E. VE-cadherin and endothelial adherens junctions: active guardians of vascular integrity. *Dev Cell*. 2013;26:441-54.
22. Noels H, Weber C and Koenen RR. Chemokines as Therapeutic Targets in Cardiovascular Disease. *Arterioscler Thromb Vasc Biol*. 2019;39:583-592.
23. Mestas J and Ley K. Monocyte-endothelial cell interactions in the development of atherosclerosis. *Trends Cardiovasc Med*. 2008;18:228-32.
24. Furchgott RF. Endothelium-Derived Relaxing Factor: Discovery, Early Studies, and Identification as Nitric Oxide (Nobel Lecture). *Angew Chem Int Ed Engl*. 1999;38:1870-1880.
25. Pober JS and Sessa WC. Evolving functions of endothelial cells in inflammation. *Nat Rev Immunol*. 2007;7:803-15.
26. Sawdey MS and Loskutoff DJ. Regulation of murine type 1 plasminogen activator inhibitor gene expression in vivo. Tissue specificity and induction by lipopolysaccharide, tumor necrosis factor-alpha, and transforming growth factor-beta. *J Clin Invest*. 1991;88:1346-53.
27. Levin EG and Loskutoff DJ. Cultured bovine endothelial cells produce both urokinase and tissue-type plasminogen activators. *J Cell Biol*. 1982;94:631-6.
28. Nachman RL and Raffi S. Platelets, petechiae, and preservation of the vascular wall. *N Engl J Med*. 2008;359:1261-70.
29. Walker AE, Henson GD, Reihl KD, Morgan RG, Dobson PS, Nielson EI, Ling J, Mechem RP, Li DY, Lesniewski LA and Donato AJ. Greater impairments in cerebral artery compared with

skeletal muscle feed artery endothelial function in a mouse model of increased large artery stiffness. *J Physiol.* 2015;593:1931-43.

30. Heiss C, Rodriguez-Mateos A and Kelm M. Central role of eNOS in the maintenance of endothelial homeostasis. *Antioxid Redox Signal.* 2015;22:1230-42.
31. Boger RH, Bode-Boger SM, Sydow K, Heistad DD and Lentz SR. Plasma concentration of asymmetric dimethylarginine, an endogenous inhibitor of nitric oxide synthase, is elevated in monkeys with hyperhomocyst(e)inemia or hypercholesterolemia. *Arteriosclerosis, thrombosis, and vascular biology.* 2000;20:1557-64.
32. Jang JJ, Ho HK, Kwan HH, Fajardo LF and Cooke JP. Angiogenesis is impaired by hypercholesterolemia: role of asymmetric dimethylarginine. *Circulation.* 2000;102:1414-9.
33. Peterson TE, Poppa V, Ueba H, Wu A, Yan C and Berk BC. Opposing effects of reactive oxygen species and cholesterol on endothelial nitric oxide synthase and endothelial cell caveolae. *Circ Res.* 1999;85:29-37.
34. Chen LY, Mehta P and Mehta JL. Oxidized LDL decreases L-arginine uptake and nitric oxide synthase protein expression in human platelets: relevance of the effect of oxidized LDL on platelet function. *Circulation.* 1996;93:1740-6.
35. Martinez-Gonzalez J, Raposo B, Rodriguez C and Badimon L. 3-hydroxy-3-methylglutaryl coenzyme a reductase inhibition prevents endothelial NO synthase downregulation by atherogenic levels of native LDLs: balance between transcriptional and posttranscriptional regulation. *Arteriosclerosis, thrombosis, and vascular biology.* 2001;21:804-9.
36. Maas R, Schwedhelm E, Kahl L, Li H, Benndorf R, Luneburg N, Forstermann U and Boger RH. Simultaneous assessment of endothelial function, nitric oxide synthase activity, nitric oxide-mediated signaling, and oxidative stress in individuals with and without hypercholesterolemia. *Clin Chem.* 2008;54:292-300.
37. Corretti MC, Anderson TJ, Benjamin EJ, Celermajer D, Charbonneau F, Creager MA, Deanfield J, Drexler H, Gerhard-Herman M, Herrington D, Vallance P, Vita J, Vogel R and International Brachial Artery Reactivity Task F. Guidelines for the ultrasound assessment of endothelial-dependent flow-mediated vasodilation of the brachial artery: a report of the International Brachial Artery Reactivity Task Force. *J Am Coll Cardiol.* 2002;39:257-65.
38. Harris RA, Nishiyama SK, Wray DW and Richardson RS. Ultrasound assessment of flow-mediated dilation. *Hypertension.* 2010;55:1075-85.
39. Holder SM, Bruno RM, Shkredova DA, Dawson EA, Jones H, Hopkins ND, Hopman MTE, Bailey TG, Coombes JS, Askew CD, Naylor L, Maiorana A, Ghiadoni L, Thompson A, Green DJ

and Thijssen DHJ. Reference Intervals for Brachial Artery Flow-Mediated Dilation and the Relation With Cardiovascular Risk Factors. *Hypertension*. 2021;77:1469-1480.

40. Celermajer DS, Sorensen KE, Bull C, Robinson J and Deanfield JE. Endothelium-dependent dilation in the systemic arteries of asymptomatic subjects relates to coronary risk factors and their interaction. *J Am Coll Cardiol*. 1994;24:1468-74.

41. Anderson TJ. Prognostic significance of brachial flow-mediated vasodilation. *Circulation*. 2007;115:2373-5.

42. Thijssen DH, Black MA, Pyke KE, Padilla J, Atkinson G, Harris RA, Parker B, Widlansky ME, Tschakovsky ME and Green DJ. Assessment of flow-mediated dilation in humans: a methodological and physiological guideline. *Am J Physiol Heart Circ Physiol*. 2011;300:H2-12.

43. Bots ML, Westerink J, Rabelink TJ and de Koning EJ. Assessment of flow-mediated vasodilatation (FMD) of the brachial artery: effects of technical aspects of the FMD measurement on the FMD response. *Eur Heart J*. 2005;26:363-8.

44. Ference BA, Ginsberg HN, Graham I, Ray KK, Packard CJ, Bruckert E, Hegele RA, Krauss RM, Raal FJ, Schunkert H, Watts GF, Boren J, Fazio S, Horton JD, Masana L, Nicholls SJ, Nordestgaard BG, van de Sluis B, Taskinen MR, Tokgozoglu L, Landmesser U, Laufs U, Wiklund O, Stock JK, Chapman MJ and Catapano AL. Low-density lipoproteins cause atherosclerotic cardiovascular disease. 1. Evidence from genetic, epidemiologic, and clinical studies. A consensus statement from the European Atherosclerosis Society Consensus Panel. *European heart journal*. 2017;38:2459-2472.

45. Baigent C, Keech A, Kearney PM, Blackwell L, Buck G, Pollicino C, Kirby A, Sourjina T, Peto R, Collins R, Simes R and Cholesterol Treatment Trialists C. Efficacy and safety of cholesterol-lowering treatment: prospective meta-analysis of data from 90,056 participants in 14 randomised trials of statins. *Lancet*. 2005;366:1267-78.

46. Boren J, Chapman MJ, Krauss RM, Packard CJ, Bentzon JF, Binder CJ, Daemen MJ, Demer LL, Hegele RA, Nicholls SJ, Nordestgaard BG, Watts GF, Bruckert E, Fazio S, Ference BA, Graham I, Horton JD, Landmesser U, Laufs U, Masana L, Pasterkamp G, Raal FJ, Ray KK, Schunkert H, Taskinen MR, van de Sluis B, Wiklund O, Tokgozoglu L, Catapano AL and Ginsberg HN. Low-density lipoproteins cause atherosclerotic cardiovascular disease: pathophysiological, genetic, and therapeutic insights: a consensus statement from the European Atherosclerosis Society Consensus Panel. *European heart journal*. 2020.

47. Cannon CP, Blazing MA, Giugliano RP, McCagg A, White JA, Theroux P, Darius H, Lewis BS, Ophuis TO, Jukema JW, De Ferrari GM, Ruzyllo W, De Lucca P, Im K, Bohula EA, Reist C, Wiviott SD, Tershakovec AM, Musliner TA, Braunwald E, Califf RM and Investigators I-I.

Ezetimibe Added to Statin Therapy after Acute Coronary Syndromes. *The New England journal of medicine*. 2015;372:2387-97.

48. Giugliano RP, Pedersen TR, Park JG, De Ferrari GM, Gaciong ZA, Ceska R, Toth K, Gouni-Berthold I, Lopez-Miranda J, Schiele F, Mach F, Ott BR, Kanevsky E, Pineda AL, Somaratne R, Wasserman SM, Keech AC, Sever PS and Sabatine MS. Clinical efficacy and safety of achieving very low LDL-cholesterol concentrations with the PCSK9 inhibitor evolocumab: a prespecified secondary analysis of the FOURIER trial. *Lancet*. 2017;390:1962-1971.
49. Schwartz GG, Steg PG, Szarek M, Bhatt DL, Bittner VA, Diaz R, Edelberg JM, Goodman SG, Hanotin C, Harrington RA, Jukema JW, Lecorps G, Mahaffey KW, Moryusef A, Pordy R, Quintero K, Roe MT, Sasiela WJ, Tamby JF, Tricoci P, White HD and Zeiher AM. Alirocumab and Cardiovascular Outcomes after Acute Coronary Syndrome. *The New England journal of medicine*. 2018;379:2097-2107.
50. Rosenson RS, Hegele RA, Fazio S and Cannon CP. The Evolving Future of PCSK9 Inhibitors. *Journal of the American College of Cardiology*. 2018;72:314-329.
51. Gaudet D, Lopez-Sendon JL, Averna M, Bigot G, Banach M, Letierce A, Loy M, Samuel R, Manvelian G, Batsu I and Henry P. Safety and efficacy of alirocumab in a real-life setting: the ODYSSEY APPRISE study. *European journal of preventive cardiology*. 2020.
52. Nicholls SJ, Puri R, Anderson T, Ballantyne CM, Cho L, Kastelein JJ, Koenig W, Somaratne R, Kassahun H, Yang J, Wasserman SM, Scott R, Ungi I, Podolec J, Ophuis AO, Cornel JH, Borgman M, Brennan DM and Nissen SE. Effect of Evolocumab on Progression of Coronary Disease in Statin-Treated Patients: The GLAGOV Randomized Clinical Trial. *JAMA*. 2016;316:2373-2384.
53. Nicholls SJ, Puri R, Anderson T, Ballantyne CM, Cho L, Kastelein JJP, Koenig W, Somaratne R, Kassahun H, Yang J, Wasserman SM, Honda S, Shishikura D, Scherer DJ, Borgman M, Brennan DM, Wolski K and Nissen SE. Effect of Evolocumab on Coronary Plaque Composition. *Journal of the American College of Cardiology*. 2018;72:2012-2021.
54. Raber L, Ueki Y, Otsuka T, Losdat S, Haner JD, Lonborg J, Fahrni G, Iglesias JF, van Geuns RJ, Ondracek AS, Radu Juul Jensen MD, Zanchin C, Stortecky S, Spirk D, Siontis GCM, Saleh L, Matter CM, Daemen J, Mach F, Heg D, Windecker S, Engstrom T, Lang IM, Koskinas KC and collaborators P-A. Effect of Alirocumab Added to High-Intensity Statin Therapy on Coronary Atherosclerosis in Patients With Acute Myocardial Infarction: The PACMAN-AMI Randomized Clinical Trial. *JAMA*. 2022;327:1771-1781.
55. Pradhan A, Kuka R, Vishwakarma P, Ali W, Perrone MA, Iellamo F, Chaudhary G, Chandra S, Sethi R, Dwivedi S, Narain V and Saran RK. Lipid Profile and Small Dense Low-

- Density Lipoprotein in Acute Coronary Syndrome Patients: Relationships to Demographic, Clinical, Angiographic, and Therapeutic Variables. *J Clin Med.* 2022;11.
56. Everett BM, Glynn RJ, MacFadyen JG and Ridker PM. Rosuvastatin in the prevention of stroke among men and women with elevated levels of C-reactive protein: justification for the Use of Statins in Prevention: an Intervention Trial Evaluating Rosuvastatin (JUPITER). *Circulation.* 2010;121:143-50.
57. Silverman MG, Ference BA, Im K, Wiviott SD, Giugliano RP, Grundy SM, Braunwald E and Sabatine MS. Association Between Lowering LDL-C and Cardiovascular Risk Reduction Among Different Therapeutic Interventions: A Systematic Review and Meta-analysis. *JAMA.* 2016;316:1289-97.
58. Correction to: PCSK9 (Proprotein Convertase Subtilisin/Kexin 9) Enhances Platelet Activation, Thrombosis, and Myocardial Infarct Expansion by Binding to Platelet CD36. *Circulation.* 2021;143:e4.
59. Qi Z, Hu L, Zhang J, Yang W, Liu X, Jia D, Yao Z, Chang L, Pan G, Zhong H, Luo X, Yao K, Sun A, Qian J, Ding Z and Ge J. PCSK9 (Proprotein Convertase Subtilisin/Kexin 9) Enhances Platelet Activation, Thrombosis, and Myocardial Infarct Expansion by Binding to Platelet CD36. *Circulation.* 2021;143:45-61.
60. Camera M, Rossetti L, Barbieri SS, Zanotti I, Canciani B, Trabattoni D, Ruscica M, Tremoli E and Ferri N. PCSK9 as a Positive Modulator of Platelet Activation. *Journal of the American College of Cardiology.* 2018;71:952-954.
61. Pirillo A, Garlaschelli K, Arca M, Averna M, Bertolini S, Calandra S, Tarugi P and Catapano AL. Spectrum of mutations in Italian patients with familial hypercholesterolemia: New results from the LIPIGEN study. *Atheroscler Suppl.* 2017;29:17-24.
62. Stitzel NO, Peloso GM, Abifadel M, Cefalu AB, Fouchier S, Motazacker MM, Tada H, Larach DB, Awan Z, Haller JF, Pullinger CR, Varret M, Rabes JP, Noto D, Tarugi P, Kawashiri MA, Nohara A, Yamagishi M, Risman M, Deo R, Ruel I, Shendure J, Nickerson DA, Wilson JG, Rich SS, Gupta N, Farlow DN, Neale BM, Daly MJ, Kane JP, Freeman MW, Genest J, Rader DJ, Mabuchi H, Kastelein JJ, Hovingh GK, Averna MR, Gabriel S, Boileau C and Kathiresan S. Exome sequencing in suspected monogenic dyslipidemias. *Circulation Cardiovascular genetics.* 2015;8:343-50.
63. Di Taranto MD, Staiano A, D'Agostino MN, D'Angelo A, Bloise E, Morgante A, Marotta G, Gentile M, Rubba P and Fortunato G. Association of USF1 and APOA5 polymorphisms with familial combined hyperlipidemia in an Italian population. *Molecular and cellular probes.* 2015;29:19-24.

64. Di Taranto MD, Benito-Vicente A, Giacobbe C, Uribe KB, Rubba P, Etxebarria A, Guardamagna O, Gentile M, Martin C and Fortunato G. Identification and in vitro characterization of two new PCSK9 Gain of Function variants found in patients with Familial Hypercholesterolemia. *Scientific reports*. 2017;7:15282.
65. Ruotolo A, Di Taranto MD, D'Agostino MN, Marotta G, Gentile M, Nunziata M, Sodano M, Di Noto R, Del Vecchio L, Rubba P and Fortunato G. The novel variant p.Ser465Leu in the PCSK9 gene does not account for the decreased LDLR activity in members of a FH family. *Clinical chemistry and laboratory medicine*. 2014;52:e175-8.
66. Hoefner DM, Hodel SD, O'Brien JF, Branum EL, Sun D, Meissner I and McConnell JP. Development of a rapid, quantitative method for LDL subfractionation with use of the Quantimetrix Lipoprint LDL System. *Clin Chem*. 2001;47:266-74.
67. Gentile M, Panico S, Mattiello A, Ubaldi S, Iannuzzo G, De Michele M, Iannuzzi A and Rubba P. Association between small dense LDL and early atherosclerosis in a sample of menopausal women. *Clin Chim Acta*. 2013;426:1-5.
68. Bonetti PO, Pumper GM, Higano ST, Holmes DR, Jr., Kuvin JT and Lerman A. Noninvasive identification of patients with early coronary atherosclerosis by assessment of digital reactive hyperemia. *Journal of the American College of Cardiology*. 2004;44:2137-41.
69. Bianchini E, Bozec E, Gemignani V, Faita F, Giannarelli C, Ghiadoni L, Demi M, Boutouyrie P and Laurent S. Assessment of carotid stiffness and intima-media thickness from ultrasound data: comparison between two methods. *J Ultrasound Med*. 2010;29:1169-75.
70. Laurent S, Cockcroft J, Van Bortel L, Boutouyrie P, Giannattasio C, Hayoz D, Pannier B, Vlachopoulos C, Wilkinson I, Struijker-Boudier H and European Network for Non-invasive Investigation of Large A. Expert consensus document on arterial stiffness: methodological issues and clinical applications. *European heart journal*. 2006;27:2588-605.
71. Laurent S, Caviezel B, Beck L, Girerd X, Billaud E, Boutouyrie P, Hoeks A and Safar M. Carotid artery distensibility and distending pressure in hypertensive humans. *Hypertension*. 1994;23:878-83.
72. Liaw A and Wiener M. Classification and Regression by randomForest. *R News*. 2002;2/3:18-22.
73. Dunn WB, Broadhurst D, Begley P, Zelena E, Francis-McIntyre S, Anderson N, Brown M, Knowles JD, Halsall A, Haselden JN, Nicholls AW, Wilson ID, Kell DB, Goodacre R and Human Serum Metabolome C. Procedures for large-scale metabolic profiling of serum and plasma using gas chromatography and liquid chromatography coupled to mass spectrometry. *Nat Protoc*. 2011;6:1060-83.

74. Ritchie ME, Phipson B, Wu D, Hu Y, Law CW, Shi W and Smyth GK. limma powers differential expression analyses for RNA-sequencing and microarray studies. *Nucleic Acids Res.* 2015;43:e47.
75. Gardner CD, Fortmann SP and Krauss RM. Association of small low-density lipoprotein particles with the incidence of coronary artery disease in men and women. *JAMA.* 1996;276:875-81.
76. St-Pierre AC, Cantin B, Dagenais GR, Mauriege P, Bernard PM, Despres JP and Lamarche B. Low-density lipoprotein subfractions and the long-term risk of ischemic heart disease in men: 13-year follow-up data from the Quebec Cardiovascular Study. *Arteriosclerosis, thrombosis, and vascular biology.* 2005;25:553-9.
77. Di Minno MN, Cavalca V, D'Angelo A, Squellerio I, Coppola A, Tremoli E and Di Minno G. Urinary excretion of iPF(2alpha)-III predicts the risk of future thrombotic events. A 10-year follow-up. *Thromb Res.* 2012;129:208-11.
78. Gentile M, Iannuzzo G, Mattiello A, Marotta G, Iannuzzi A, Panico S and Rubba P. Association between Lp (a) and atherosclerosis in menopausal women without metabolic syndrome. *Biomark Med.* 2016;10:397-402.
79. Burgess S, Ference BA, Staley JR, Freitag DF, Mason AM, Nielsen SF, Willeit P, Young R, Surendran P, Karthikeyan S, Bolton TR, Peters JE, Kamstrup PR, Tybjaerg-Hansen A, Benn M, Langsted A, Schnohr P, Vedel-Krogh S, Kobylecki CJ, Ford I, Packard C, Trompet S, Jukema JW, Sattar N, Di Angelantonio E, Saleheen D, Howson JMM, Nordestgaard BG, Butterworth AS, Danesh J, European Prospective Investigation Into C and Nutrition-Cardiovascular Disease C. Association of LPA Variants With Risk of Coronary Disease and the Implications for Lipoprotein(a)-Lowering Therapies: A Mendelian Randomization Analysis. *JAMA Cardiol.* 2018;3:619-627.
80. Romagnuolo R, DeMarco K, Scipione CA, Boffa MB and Koschinsky ML. Apolipoprotein(a) inhibits the conversion of Glu-plasminogen to Lys-plasminogen on the surface of vascular endothelial and smooth muscle cells. *Thromb Res.* 2018;169:1-7.
81. Marston NA, Gurm Y, Melloni GEM, Bonaca M, Gencer B, Sever PS, Pedersen TR, Keech AC, Roselli C, Lubitz SA, Ellinor PT, O'Donoghue ML, Giugliano RP, Ruff CT and Sabatine MS. The Effect of PCSK9 (Proprotein Convertase Subtilisin/Kexin Type 9) Inhibition on the Risk of Venous Thromboembolism. *Circulation.* 2020;141:1600-1607.
82. Nicholls SJ, Brandrup-Wognsen G, Palmer M and Barter PJ. Meta-analysis of comparative efficacy of increasing dose of Atorvastatin versus Rosuvastatin versus Simvastatin on lowering levels of atherogenic lipids (from VOYAGER). *Am J Cardiol.* 2010;105:69-76.

83. Vlachopoulos C, Aznaouridis K, Dagher A, Vasiliadou C, Masoura C, Stefanadi E, Skoumas J, Pitsavos C and Stefanadis C. Protective effect of atorvastatin on acute systemic inflammation-induced endothelial dysfunction in hypercholesterolaemic subjects. *European heart journal*. 2007;28:2102-9.
84. Gong X, Ma Y, Ruan Y, Fu G and Wu S. Long-term atorvastatin improves age-related endothelial dysfunction by ameliorating oxidative stress and normalizing eNOS/iNOS imbalance in rat aorta. *Exp Gerontol*. 2014;52:9-17.
85. Hilvo M, Simolin H, Metso J, Ruuth M, Oorni K, Jauhiainen M, Laaksonen R and Baruch A. PCSK9 inhibition alters the lipidome of plasma and lipoprotein fractions. *Atherosclerosis*. 2018;269:159-165.
86. Janis MT, Tarasov K, Ta HX, Suoniemi M, Ekroos K, Hurme R, Lehtimäki T, Paiva H, Kleber ME, Marz W, Prat A, Seidah NG and Laaksonen R. Beyond LDL-C lowering: distinct molecular sphingolipids are good indicators of proprotein convertase subtilisin/kexin type 9 (PCSK9) deficiency. *Atherosclerosis*. 2013;228:380-5.
87. Tarasov K, Ekroos K, Suoniemi M, Kauhanen D, Sylvanne T, Hurme R, Gouni-Berthold I, Berthold HK, Kleber ME, Laaksonen R and Marz W. Molecular lipids identify cardiovascular risk and are efficiently lowered by simvastatin and PCSK9 deficiency. *J Clin Endocrinol Metab*. 2014;99:E45-52.
88. Laaksonen R, Ekroos K, Sysi-Aho M, Hilvo M, Vihervaara T, Kauhanen D, Suoniemi M, Hurme R, Marz W, Scharnagl H, Stojakovic T, Vlachopoulou E, Lokki ML, Nieminen MS, Klingenberg R, Matter CM, Hornemann T, Juni P, Rodondi N, Raber L, Windecker S, Gencer B, Pedersen ER, Tell GS, Nygard O, Mach F, Sinisalo J and Luscher TF. Plasma ceramides predict cardiovascular death in patients with stable coronary artery disease and acute coronary syndromes beyond LDL-cholesterol. *European heart journal*. 2016;37:1967-76.
89. Taniguchi M and Okazaki T. The role of sphingomyelin and sphingomyelin synthases in cell death, proliferation and migration-from cell and animal models to human disorders. *Biochim Biophys Acta*. 2014;1841:692-703.
90. Mu H, Wang X, Wang H, Lin P, Yao Q and Chen C. Lactosylceramide promotes cell migration and proliferation through activation of ERK1/2 in human aortic smooth muscle cells. *Am J Physiol Heart Circ Physiol*. 2009;297:H400-8.
91. Li Z, Fan Y, Liu J, Li Y, Huan C, Bui HH, Kuo MS, Park TS, Cao G and Jiang XC. Impact of sphingomyelin synthase 1 deficiency on sphingolipid metabolism and atherosclerosis in mice. *Arteriosclerosis, thrombosis, and vascular biology*. 2012;32:1577-84.

92. Boren J and Williams KJ. The central role of arterial retention of cholesterol-rich apolipoprotein-B-containing lipoproteins in the pathogenesis of atherosclerosis: a triumph of simplicity. *Curr Opin Lipidol.* 2016;27:473-83.
93. Kitatani K, Nemoto M, Akiba S and Sato T. Stimulation by de novo-synthesized ceramide of phospholipase A(2)-dependent cholesterol esterification promoted by the uptake of oxidized low-density lipoprotein in macrophages. *Cell Signal.* 2002;14:695-701.
94. Hashizume T, Kitatani K, Kageura T, Hayama M, Akiba S and Sato T. Ceramide enhances susceptibility of membrane phospholipids to phospholipase A2 through modification of lipid organization in platelet membranes. *Biol Pharm Bull.* 1999;22:1275-8.
95. Sato T, Kageura T, Hashizume T, Hayama M, Kitatani K and Akiba S. Stimulation by ceramide of phospholipase A2 activation through a mechanism related to the phospholipase C-initiated signaling pathway in rabbit platelets. *J Biochem.* 1999;125:96-102.
96. Rhoads JP and Major AS. How Oxidized Low-Density Lipoprotein Activates Inflammatory Responses. *Crit Rev Immunol.* 2018;38:333-342.
97. Majtan T, Pey AL, Gimenez-Mascarell P, Martinez-Cruz LA, Szabo C, Kozich V and Kraus JP. Potential Pharmacological Chaperones for Cystathionine Beta-Synthase-Deficient Homocystinuria. *Handb Exp Pharmacol.* 2018;245:345-383.
98. Vance DE. Phospholipid methylation in mammals: from biochemistry to physiological function. *Biochim Biophys Acta.* 2014;1838:1477-87.
99. Di Minno A, Gentile M, Iannuzzo G, Calcaterra I, Tripaldella M, Porro B, Cavalca V, Di Taranto MD, Tremoli E, Fortunato G, Rubba POF and Di Minno MND. Endothelial function improvement in patients with familial hypercholesterolemia receiving PCSK-9 inhibitors on top of maximally tolerated lipid lowering therapy. *Thrombosis Research.* 2020;194:229-236.
100. Bremer J and Greenberg DM. Methyl transferring enzyme system of microsomes in the biosynthesis of lecithin (phosphatidylcholine). *Biochimica et Biophysica Acta.* 1961;46:205-216.
101. Obeid R and Herrmann W. Homocysteine and lipids: S-adenosyl methionine as a key intermediate. *FEBS letters.* 2009;583:1215-25.
102. DeLong CJ, Shen YJ, Thomas MJ and Cui Z. Molecular distinction of phosphatidylcholine synthesis between the CDP-choline pathway and phosphatidylethanolamine methylation pathway. *J Biol Chem.* 1999;274:29683-8.
103. Fagone P and Jackowski S. Phosphatidylcholine and the CDP-choline cycle. *Biochim Biophys Acta.* 2013;1831:523-32.
104. McMaster CR. From yeast to humans - roles of the Kennedy pathway for phosphatidylcholine synthesis. *FEBS letters.* 2018;592:1256-1272.

105. Resseguie ME, da Costa KA, Galanko JA, Patel M, Davis IJ and Zeisel SH. Aberrant estrogen regulation of PEMT results in choline deficiency-associated liver dysfunction. *J Biol Chem*. 2011;286:1649-58.
106. Marcil M, Yu L, Krimbou L, Boucher B, Oram JF, Cohn JS and Genest J, Jr. Cellular cholesterol transport and efflux in fibroblasts are abnormal in subjects with familial HDL deficiency. *Arteriosclerosis, thrombosis, and vascular biology*. 1999;19:159-69.
107. Paciullo F, Momi S and Gresele P. PCSK9 in Haemostasis and Thrombosis: Possible Pleiotropic Effects of PCSK9 Inhibitors in Cardiovascular Prevention. *Thromb Haemost*. 2019;119:359-367.
108. Vance DE. From masochistic enzymology to mechanistic physiology and disease. *J Biol Chem*. 2017;292:17169-17177.
109. Hartroft WS, Ridout JH, Sellers EA and Best CH. Atheromatous changes in aorta, carotid and coronary arteries of choline-deficient rats. *Proc Soc Exp Biol Med*. 1952;81:384-93.
110. Vance JE and Vance DE. The role of phosphatidylcholine biosynthesis in the secretion of lipoproteins from hepatocytes. *Can J Biochem Cell Biol*. 1985;63:870-81.
111. Zhao Y, Su B, Jacobs RL, Kennedy B, Francis GA, Waddington E, Brosnan JT, Vance JE and Vance DE. Lack of phosphatidylethanolamine N-methyltransferase alters plasma VLDL phospholipids and attenuates atherosclerosis in mice. *Arteriosclerosis, thrombosis, and vascular biology*. 2009;29:1349-55.
112. Brown SL, Jala VR, Raghuwanshi SK, Nasser MW, Haribabu B and Richardson RM. Activation and regulation of platelet-activating factor receptor: role of G(i) and G(q) in receptor-mediated chemotactic, cytotoxic, and cross-regulatory signals. *J Immunol*. 2006;177:3242-9.
113. Lordan R, Tsoupras A and Zabetakis I. Platelet activation and prothrombotic mediators at the nexus of inflammation and atherosclerosis: Potential role of antiplatelet agents. *Blood Rev*. 2020:100694.
114. Karasawa K and Inoue K. Overview of PAF-Degrading Enzymes. *Enzymes*. 2015;38:1-22.
115. Palur Ramakrishnan AV, Varghese TP, Vanapalli S, Nair NK and Mingate MD. Platelet activating factor: A potential biomarker in acute coronary syndrome? *Cardiovasc Ther*. 2017;35:64-70.
116. Pastori D, Nocella C, Farcomeni A, Bartimoccia S, Santulli M, Vasaturo F, Carnevale R, Menichelli D, Violi F, Pignatelli P and Group A-AS. Relationship of PCSK9 and Urinary Thromboxane Excretion to Cardiovascular Events in Patients With Atrial Fibrillation. *Journal of the American College of Cardiology*. 2017;70:1455-1462.

117. Koskinas KC, Windecker S, Buhayer A, Gencer B, Pedrazzini G, Mueller C, Cook S, Muller O, Matter CM, Raber L, Heg D, Mach F and Investigators E. Design of the randomized, placebo-controlled evolocumab for early reduction of LDL-cholesterol levels in patients with acute coronary syndromes (EVOPACS) trial. *Clin Cardiol.* 2018;41:1513-1520.
118. Dubuc G, Chamberland A, Wassef H, Davignon J, Seidah NG, Bernier L and Prat A. Statins upregulate PCSK9, the gene encoding the proprotein convertase neural apoptosis-regulated convertase-1 implicated in familial hypercholesterolemia. *Arteriosclerosis, thrombosis, and vascular biology.* 2004;24:1454-9.